Mechanisms and Evolution of Magnetotactic Bacteria

Thesis by

Cody Nash

In Partial Fulfillment of the Requirements

for the Degree of

Doctor of Philosophy

California Institute of Technology

Pasadena, California

2008

(Defended May 22, 2008)

Acknowledgements

I would like to thank first and foremost, my advisor, Joseph Kirschvink. Without his support and encouragement I couldn't have done this. Joe exemplifies the finest quality of a scientist — the ability to get others excited about learning. I thank Bob Kopp for being a friend and for the engaging discussions and so much assistance with learning magnetometry. It was through Bob's recognition that he could use some of my discoveries for his own work that I began to understand how I could contribute as a scientist.

I thank Arash Komeili and Betty Bertani for teaching me everything I know about genetics. I would like to thank Dianne Newman for letting me be a part of her lab, and Victoria Orphan and Ken Nealson for giving me the opportunity to work in their labs as well.

Quite a number of people have assisted me over the years in my field work, which is yet another chapter in Joe's quest to find a magnetotactic Archaea. Before I got here Megan Andrews laid the groundwork, and countless Ge1 students over the decades have gone with Joe to Mono Lake to search for unusual bacteria. None of this would have been possible without assistance from Tom Crowe, SNARL, and Dan Dillingess for providing boating, sampling, and SCUBA expertise regarding Mono Lake. I thank Clint Dodd, Michael Shearn, and M. David Henry for helping me re-acquaint myself with SCUBA. I want to thank Radu Popa for his assistance over the years on this project. Along the way Radu and I discovered thermophilic magnetotactic bacteria and he has let me run with it.

I also want to thank Mom for never giving up on me, my father and grandparents who saw me start this journey, Patty and Robert for being family through it all, Elizabeth Bent who made so many problems smaller, Sara Egner who always cheered me up, and last but not least Dala, who never left me alone.

Abstract (350 Words)

Magnetotactic bacteria (MB) contain intracellular magnetic crystals of iron oxides and/or iron sulfides. These crystals and the membranes which enclose them are together known as magnetosomes. The crystals formed by MB fall into a narrow size range and have species-specific crystal morphologies. Magnetosomes are physically connected to the rest of the cell by actin-like filaments that are thought to allow the MB to take advantage of their passive orientation in the Earth's magnetic field to navigate more efficiently across chemical gradients. The large excess of crystals in most strains suggests that magnetosomes may also function as an iron reservoir or as a redox battery.

This thesis describes a number of investigations of the MB. First, a set of genes was identified as being conserved uniquely among the MB by comparative genomics. This method was validated by finding many of the genes already known to be involved in magnetotaxis. Many additional genes were identified and some of these genes were found to cluster together. Three of these clusters were genetically interrupted to determine their role in magnetite biomineralization.

Second, a transposon mutagenesis was undertaken to identify genes necessary for the magnetic phenotype of MB. Out of 5809 mutants screened, nineteen were found to be non- or partially magnetic. Fourteen of these have insertion sites in genes known to be involved in magnetotaxis. Five more were found to have insertions in previously unsuspected genes. The mutant phenotypes of the five mutants include the complete absence of magnetosomes, elongate crystals, reduced numbers of crystals and incomplete mineralization. These mutant strains were used to develop ferromagnetic resonance theory of isolated single-domain particles and biogenic particle identification.

Third, MB were discovered in hot springs and in hyper-saline, hyper-alkaline Mono Lake, CA. This extends the environmental range of MB to astro- and paleobiologically relevant environments. Magnetotactic Archaea were tentatively identified from Mono Lake, CA and are the first magnetotactic representatives of that domain.

Table of Contents

Summary

This thesis set out to be an exploration of the magnetotactic bacteria. Going into it my interests were evolutionary and planetary. How long had magnetotactic bacteria been around? Which planet did they come from? The advent of nanotechnology in society made me wonder what technologies could be enabled by understanding how magnetotactic bacteria make their crystals. Could we make a better battery? Or a better hard drive? How about better contrast agents for magnetic resonance imaging? Or better standards for basic research in magnetism? Along the way through graduate school I became aware of the ways in which magnetotactic bacteria can be of use in geobiological investigations. The preservation of the crystals from the magnetosomes in the rock record summons dreams of a bacterial fossil record — a new set of calibration points for our evolutionary models. Their efficient migration back and forth through redox gradients means they may be important in the cycling of the iron, sulfur, phosphorus, and nitrates that are found stored in most of them. And really so little is known about them. Can they use the iron in their magnetosomes for other cellular processes?

So I began by looking at the genomes of the magnetotactic bacteria, looking to see which genes are correlated with the magnetotactic phenotype. After finding a far larger set than expected, I began genetic manipulations of the genes predicted by the genomic analysis. The targeted interruption of three different operons resulted in no significant effect. This may be because the genes are not involved in the magnetic phenotype, but could be due to a number of other reasons. The genes may not be necessary under the conditions assayed or the interruptions may not have disrupted the

expression of downstream genes which are necessary. This work constitutes the first chapter of my thesis.

Then I learned about transposon mutagenesis and set out to see how many genes could be discovered by randomly knocking them out. This is the work presented in Chapter 2. This work consisted of generating 5809 mutants and screening them with a magnetic and PCR assay to detect non-magnetic mutants that weren't due to the spontaneous loss of the mamAB cluster. Nineteen non-magnetic mutants were found, five of which have transposon insertion sites in genes outside the mam clusters. These five mutants are insertions in a predicted radical SAM protein, a hydrolase, a transcriptional regulator, an indole-pyruvate oxidoreductase, and a hypothetical protein. Their phenotypes are, respectively, no magnetosome vesicles, elongate crystals, fewer crystals, 1–2 crystals, and poorly formed crystals. Two of the mutants were the subject of additional work described in the appendices.

Finally, two studies concerning magnetotactic bacteria in the environment are presented in Chapter 3. The first documents a search for magnetotactic archaea, for which the first sequences are presented. In the course of this search we discovered MB for the first time in hot springs and present the first work describing MB from the hyper-saline, hyper-alkaline Mono Lake, CA. This extends the relevance of MB to the geo- and astrobiologically relevant environments of geothermal features and ancient, evaporitic basins. Also presented is the first fragment of a gene known to be involved in magnetotaxis from the environment — part of the *mamB* gene recovered from magnetic cocci in the LA arboretum using magnetic column purification and degenerate primers.

Chapter One: Genomics

1.1. Comparative genomics of the MS-1 and MC-1 genome

Abstract

The biologically controlled mineralization of magnetite (BCMM) within lipid-bilayer-bounded vesicles (magnetosomes) by some bacteria is the biophysical basis of their magnetotactic behavior and is under genetic control. In an effort to identify genes involved in this process we compared the genomes of two magnetotactic bacteria, *Magnetospirillum magnetotacticum* MS-1 and magnetic coccus strain MC-1, to each other and to the NCBI protein database. Our comparison focused on finding proteins conserved particularly between these magnetotactic bacteria. We define a conserved gene in MS-1 as a gene (i.e., gene A) with the highest sequence similarity to a gene from MC-1, gene B, where gene B also best matches a gene from MS-1. In MS-1 and MC-1 we found 115 and 91 conserved open reading frames (ORFs), respectively, showing that the two species use similar systems for BCMM. The conserved ORFs include 15 of the 20 genes whose products are reported to localize to the magnetosome [*Grünberg et al.*, 2004] and 2 of the 3 genes reported to be involved in BCMM based on transposon mutagenesis studies [*Komeili et al.*, 2004; *Nakamura et al.*, 1995]. They also include a significant number of ORFs involved in functions consistent with models of magnetotaxis, including glycoprotein synthesis, redox reactions, inorganic ion transport, and signal transduction. We elaborate upon previous models of magnetotaxis with pathways deduced from the conserved ORFs and find support for the hypothesis that BCMM is a metabolic strategy as well as a navigational one.

1.1.1. Introduction

The highly defined nature of biologically controlled mineralization of magnetite (BCMM) implies strict genetic control, especially as no abiological method for synthesizing such particles has been discovered after decades of industrial and scientific effort [*Thomas-Keprta et al.*, 2000]. Modern bacterial BCMM produces magnetite as individual crystals bound within lipid-bilayer membranes (magnetosomes) and organized into chains [*Balkwill et al.*, 1980]. Magnetosome chains are thought to be used to take advantage of the Earth's magnetic field for navigation of chemical gradients [*Frankel and Bazylinski*, 1994; *Kirschvink*, 1980], though they may also function as a redox reservoir [*Vali and Kirschvink*, 1991], and/or be a metabolic by-product [*Guerin and Blakemore*, 1992].

The wide but sparse distribution of BCMM among the domain Bacteria suggests that it evolved multiple times [*Delong et al.*, 1993; *Kawaguchi et al.*, 1995] or has been laterally transferred. The same distribution argues against the less parsimonious hypothesis that BCMM is ancestral to the Bacteria and most bacteria have lost it. If it did evolve multiple times we would expect different genes to be involved in each system, whereas if it had been laterally transferred or was ancestral we would expect to find orthologous genes in each system. Protein separation studies indicate there are more than 18 different proteins specific to the magnetosome membrane [*Grünberg et al.*, 2004] and a transposon mutagenesis study suggests there may be as many as 60 different genes involved in BCMM [*Wahyudi et al.*, 2001]. Only a few of these genes and proteins have been characterized. Previous studies have shown many of the genes whose products appear to localize to the magnetosome membrane are part of a gene cluster present in

three different BCMM bacteria (magnetic coccus strain MC-1, *Magnetospirillum magnetotacticum* MS-1, and *M. gryphiswaldense* MSR-1) [*Grünberg et al.*, 2001; *Grünberg et al.*, 2004]. Most of the genes in this cluster are reported as having much less similarity to genes from non-BCMM organisms than to genes from other BCMM organisms (i.e., they appear conserved among BCMM organisms). The conservation of these genes among the magnetospirilla and the magnetic cocci indicates that they are using the same genetic system for BCMM.

The presence of conserved genes and gene clusters associated with the magnetosome membrane, the indication that there are many undiscovered genes involved, and the availability of the genomes of two BCMM bacteria (MS-1 and MC-1) prompted us to search these genomes for other conserved genes and clusters. We hypothesized that these genomes would contain genes that would be more similar to each other than to any other non-BCMM organism due to conserved BCMM functionality arising from a common evolutionary origin. MS-1 and MC-1 are well suited to this analysis because they share few other traits besides BCMM that they do not also share with other α-proteobacteria. They differ in habitat, cell shape, flagellar location, aerotactic behavior, magnetite crystal form, and the guanine-cytosine (GC) content of their genomes (see Table 1). They are also phylogenetically distinct based on 16S rRNA sequences, with MC-1 branching off from the base of the α-Proteobacteria and MS-1 branching off deeper within the phylum. The non-BCMM α-proteobacteria genomes in particular, as well as the rest of the Genbank database, act as a filter to identify common genes (e.g., metabolic and information processing) which are not conserved only among BCMM bacteria and thus not likely to be a unique part of the BCMM apparatus.

Table 1: Comparison of MS-1 and MC-1 Traits

Quality	MS-1	MC-1
Cell Shape	Spirillum [*Blakemore et al.*, 1979]	Coccus [*Meldrum et al.*, 1993]
Flagellar Location	Polar [*Frankel et al.*, 1997]	Bilophotrichous [*Frankel et al.*, 1997]
Aerotactic Behavior	Temporal [*Frankel et al.*, 1997]	2-Way Switch [*Frankel et al.*, 1997]
Magnetite Crystal Form	Cubo-Octahedral [*Mann et al.*, 1984]	Hexahedral [*Meldrum et al.*, 1993]
Habitat	Freshwater sediment [*Blakemore et al.*, 1979]	Estuary sediment [*Meldrum et al.*, 1993]
GC content	63.0% [*Sakane and Yokota*, 1994]	52–57% [*Dean and Bazylinski*, 1999]

Through the use of this comparative genomic strategy, called differential genome comparison [*Raymond et al.*, 2002], we have identified a set of open reading frames (ORFs) likely involved in BCMM. The validity of the technique is supported by the fact that we find most of the genes which localize to the magnetosome membrane to be conserved. Conserved metabolic ORFs support the hypothesis that BCMM is more than just a navigational strategy. Conserved glycoprotein synthesis ORFs support the hypothesis that BCMM is a matrix-vesicle type biomineralization system. This set of ORFs can act as a library of targets for future investigations of the evolution and process of BCMM.

1.1.2. Methods and Definitions

Genome comparisons were made using the blastp program of the BLAST package [*Altschul et al.*, 1997] without the simple sequence filter and with an expectancy cutoff of 10^{-5}. Translated ORF models for the MS-1 and MC-1 genomes were obtained from the National Center for Biotechnology (NCBI, www.ncbi.nih.gov). Sequences of MS-1 DNA published and deposited in Genbank earlier are 98–100% consistent with the draft sequence (data not shown). An analysis of GC content versus contig size indicates that the larger contigs have the expected composition (data not shown). We only use 316 of the 3880 available contigs, those which have 20x coverage or greater and thus have the highest sequence quality. These contigs provide > 95% coverage of the genome. Comparisons were made to Genbank's non-redundant (nr) protein database, available from the NCBI website (www.ncbi.nlm.nih.gov).

Conservancy for a given ORF was calculated as the difference in BLAST bit scores between the ORF's closest match in a given target genome and its closest match in the nr database, excluding hits to other BCMM bacteria.

A *conserved gene*, gene A, in MS-1 is defined as best matching a gene from MC-1, gene B, where gene B best matches a gene from MS-1. Conserved genes are likewise defined for MC-1.

Genes and ORFs were mapped by contig and scaffold information obtained from the DOE JGI. Note that *contigs* are fractions of the genome sequence determined from connecting overlapping sequencing runs. *Scaffolds* are sequences of oriented contigs with gaps between the contigs.

Operons were defined as a sequence of ORFs transcribed in the same direction without a gap larger than 200 base pairs between any of the ORFs.

1.1.3. Results and Discussion

1.1.3.1 Conserved ORFs and clusters

Out of 4280 ORF models in MS-1, we found 115 ORFs fitting our definition of conserved. In MC-1 we found 91 conserved ORFs out of 3677 total ORF models. The conserved ORFs are arranged in 53 clusters and operons in MS-1 (see Figure 1) and 51 clusters and operons in MC-1. A number of conserved ORFs were found in the same clusters in both genomes, with common functionality predicted in both genomes (see Table 2). Several of these clusters were duplicated in one or both of the genomes.

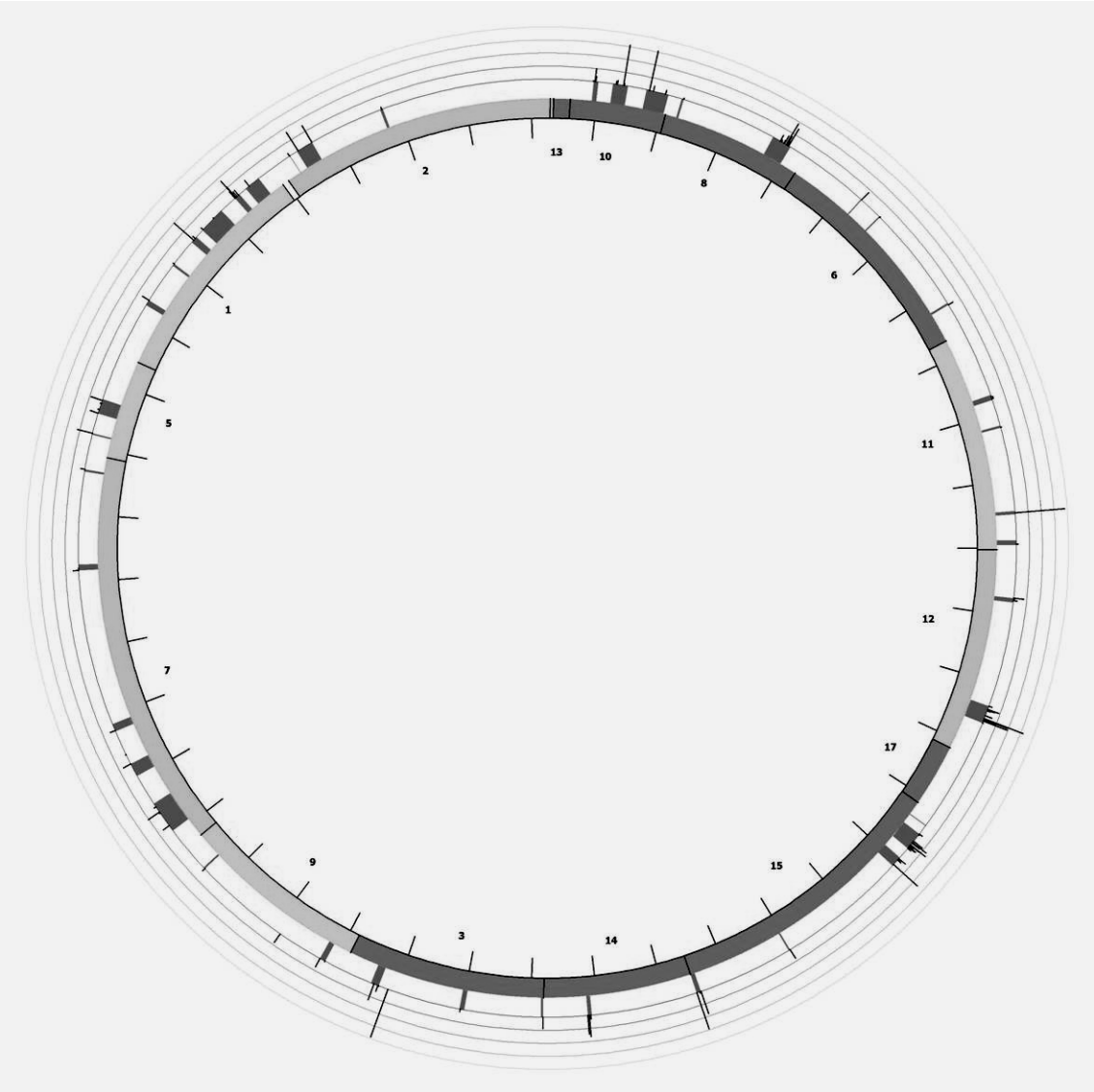

Figure 1: Map of conserved ORFs in MS-1. Spikes on the outer rim represent conserved genes, with length scaled to conservancy. Ticks represent 100kb. Scaffold position and orientation determined by restriction mapping ([*Bertani et al.*, 2001] and unpublished data).

Table 2: Conserved Clusters

MS-1 ORF	MC-1 ORF	COG	Cons
210479	2713	Hypothetical protein	26
210481	2715	Predicted carbamoyl transferase, NodU family	12
210485	3211	Glycosyltransferase	76
28368	1292	ABC-type phosphate transport system, permease component	23
28369	**1291**	ABC-type phosphate transport system, ATPase component	8
29670	184	TRAP-type C4-dicarboxylate transport system, periplasmic component	75
29671	**185**	Adenylate cyclase, family 3 (some proteins contain HAMP domain)	195
29464	916	Methyl-accepting chemotaxis protein	298
29465	915	Chemotaxis response regulator: CheY-like receiver and methylesterase	65
29466	914	Methylase of chemotaxis methyl-accepting proteins	150
29467	913	Chemotaxis protein histidine kinase and related kinases	366
29468	912	Response regulators: CheY-like receiver and winged-helix DNA-binding	49.4
29469	911	Response regulator: CheY-like receiver and a GGDEF	130
29470	910	Chemotaxis signal transduction protein	47.3
29439	1756	Thiol-disulfide isomerase and thioredoxins	17
29440	1755	Predicted permeases	60
29366	1519	Hypothetical protein	172
29367	1520	Permeases of the major facilitator superfamily	485
28051	**3295**	Membrane-fusion protein	636
28052	**3296**	Membrane-fusion protein	380
28053	**3297**	Membrane-fusion protein	135
28054	**3298**	Outer membrane protein	362
27932	**3297**	Membrane-fusion protein	17
27933	**3296**	Membrane-fusion protein	101
27934	**3295**	Membrane-fusion protein	178
27993	2747	Membrane-fusion protein	51
27994	2746	ABC-type bacteriocin/lantibiotic exporters	320
27995	2745	ABC-type bacteriocin/lantibiotic exporters	283
27944	2613	Hypothetical protein	94
27945	2612	Adenylate cyclase, family 3 (some proteins contain HAMP domain)	212
29034	281	Hypothetical protein (MamI)	79.7
29035	**267**	Trypsin-like serine proteases, typically periplasmic (MamE)	170
29037	273	Actin-like ATPase involved in cell morphogenesis (MamK)	126
29039	274	Predicted Co/Zn/Cd cation transporters (MamM)	120
29041	**275**	Predicted permeases (MamO)	283.1
29042	276	Trypsin-like serine proteases, typically periplasmic (MamP)	161
29043	277	FOG: TPR repeat (MamA)	70.7
29046	**1531**	Predicted Co/Zn/Cd cation transporters (MamB)	120
29047	1530	Hypothetical protein (MamS)	79.3
29048	1529	Cytochrome c, mono- and diheme variants (MamT)	115
29050	**1531**	Predicted Co/Zn/Cd cation transporters	41
28108	**267**	Trypsin-like serine proteases, typically periplasmic (MamE duplication)	122
28110	**275**	Trypsin-like serine proteases, typically periplasmic (MamO duplication)	41.9

The distribution of conserved ORFs among COG families is significantly different from that of a random sample of their respective genomes. Both sets of conserved ORFs contain more cell envelope biogenesis, cell motility/secretion, inorganic ion transport/metabolism, carbohydrate transport/metabolism, energy production, and signal transduction ORFs. Both sets were also deficient in housekeeping ORFs (translation and amino acid/nucleic acid/lipid metabolism).

Finding a large set of ORFs conserved particularly between MS-1 and MC-1 supports the hypothesis that they use similar mechanisms to carry out BCMM. The presence of a large number of the conserved ORFs in clusters present in both bacteria, sometimes with the order of ORFs conserved as well, and the fact that the distribution of predicted functions is non-random lends support to the hypothesis that these ORFs function together in a larger framework.

1.1.3.2. Previously documented genes

Fifteen of the genes previously cloned and sequenced from magnetotactic bacteria are found to be conserved, all of which come from the *mam* cluster (see Table 3). Two bacterioferritin genes, RubisCO, superoxide dismutase *sodB, phaZ1,* and *mms16* are not found in MC-1. The genes *magA, recA*, RNase HII, *mpsA*, cytochromes cb1, c-550 and a1, and a nitrate reductase gene cluster (*nap)* are present in both genomes but not conserved. Further, eight putative transposases located around the mam cluster in MSR-1 are either not conserved or absent from the MC-1 genome.

Table 3: Conservation of Cloned Magnetospirillum BCMM Genes

Gene	Source	MC-1 ORF	Bit Score	NR best hit	Bit Score	Cons.
MagA	AMB-1	2765	169	Unknown	264	-95
MamA	**MSR-1**	**277**	**150**	**O-linked N-acetylglucosamine transferase**	**82.8**	**67.2**
MamB	**MSR-1**	**1531**	**287**	**Cation efflux family protein**	**166**	**121**
MamC	MSR-1	269	45.1	Hypothetical protein	54.3	-9.2
MamD	**MSR-1**	**1518**	**71.2**	**Heavy-chain fibroin**	**70.1**	**1.1**
MamE	**MSR-1**	**267**	**218**	**Probable serine protease**	**168**	**50**
MamF	**MSR-1**	**283**	**81.6**	**-**	**-**	**81.6**
MamG	MSR-1	-	-	Fibroin heavy chain precursor-like protein	65.5	-65.5
MamH	**MSR-1**	**266**	**414**	**Transporter, putative**	**162**	**252**
MamI	**MSR-1**	**281**	**42**	**-**	**-**	**42**
MamJ	MSR-1	-	-	Hypothetical protein	95.9	-95.9
MamK	**MSR-1**	**273**	**357**	**Unknown**	**208**	**149**
MamL	MSR-1	-	-	-	-	-
MamM	**MSR-1**	**274**	**289**	**Predicted Co/Zn/Cd cation transporters**	**147**	**142**
MamN	MSR-1	-	-	ArsB, Arsenical pump membrane protein	189	-189
MamO	**MSR-1**	**275**	**290**	**Serine protease**	**90.9**	**199.1**
MamP	**MSR-1**	**276**	**141**	**-**	**-**	**141**
MamQ	MSR-1	1533	81.3	LemA	90.1	-8.8
MamR	MSR-1	-	-	-	-	-
MamS	**MSR-1**	**1530**	**69.3**	**-**	**-**	**69.3**
MamT	**MSR-1**	**1529**	**114**	**-**	**-**	**114**
MamU	MSR-1	-	-	Hypothetical protein	159	-159
MM22	MSR-1	-	-	Hypothetical protein	61.6	-61.6
Mms16	AMB-1	-	-	Hypothetical protein	164	-164
Mms6	**AMB-1**	-	-	Fibroin heavy chain precursor-like protein	58.9	-58.9
MpsA	AMB-1	125	308	Acetyl-CoA carboxylase alpha subunit	444	-136

The fact that the conserved ORFs contain 15 of the 25 genes reported to encode magnetosome-specific proteins supports the hypothesis that conserved ORFs are associated with BCMM. The absence of the putatively magnetosome-specific gene *mms16* from MC-1 is consistent with recent observations of Mms16's association with poly-hydroxy alkanoate metabolism as opposed to magnetosomes [*Grünberg et al.*, 2004;

Handrick et al., 2004]. The first gene shown by mutagenesis to be necessary for BCMM, *magA* [*Nakamura et al.*, 1995], is present in MC-1, but it is not conserved. MagA is an iron-transporter, so it is likely that while necessary for BCMM in MS-1, its use is not restricted to BCMM. MpsA is present in MC-1, but the *Magnetospirillum* MpsA is most similar to an acetyl-CoA carboxylase subunit from *Rhodosprillim rubrum*, arguing that the gene plays a broader role in the cell that has been exapted to BCMM in the magnetotactic bacteria.

1.1.3.3. BCMM model

The predicted functions of the conserved ORFs fit into previous models of BCMM [*Frankel et al.*, 1983; *Kirschvink and Lowenstam*, 1979; *Mann et al.*, 1990]. In these models BCMM is divided into distinct processes: magnetosome membrane formation, iron uptake, low-density ferrihydrite formation, dehydration to a higher-density ferrihydrite, and finally conversion to magnetite. We do not expect all of these processes to be conserved because they will have other uses besides BCMM such that they will be found in non-BCMM species. Iron uptake is necessary for many cellular activities, and membrane budding and formation are essential to cell division. There are several processes which we do expect to find conserved, namely controls of crystal morphology, ultrastructures for maintaining the magnetosomes in a chain, mechanisms for transport into and out of the magnetosomes, and regulatory elements for all of these activities.

1.1.3.3.1 Iron transport and redox control

Iron transport within the cell may be carried out by MagA, a known iron transporter in BCMM bacteria [*Nakamura et al.*, 1995], though it is not conserved and may not function specifically for BCMM. MagA is involved in iron-efflux, and may be widely used to prevent metals from building up to toxic levels in the cytoplasm. Both MS-1 and MC-1 have non-conserved ORFs for the *feo* ferrous iron transporter for transport across the cytoplasmic membrane as well as several non-conserved ferric uptake regulators. Conserved predicted metal transporters are found only in the *mam* cluster. In the *mam* cluster there are four conserved predicted cobalt/zinc/cadmium cation transport ORFs. Recent work has shown cobalt can be incorporated into the magnetosomes of three strains of magnetospirilla [*Staniland et al.*, 2008]. These transporters may function for iron transport in the magnetospirilla, but one or more still have retained vestigial cobalt transport capacity. One of the conserved metal transporters is the *mamB* gene, which is known to specifically localize to the magnetosome membrane. There are several other conserved ORFs and ORF clusters encoding predicted transporters, but the molecule to be transported was either non-metallic (phosphate and sulfate) or not predicted.

BCMM involves the conversion of iron to a low-density ferrihydrite through a series of metabolic reactions. Ferric iron is first reduced, a process which primarily occurs in the periplasm in MS-1, possibly as an energy-conserving process [*Guerin and Blakemore*, 1992; *Paoletti and Blakemore*, 1988] linked to magnetite synthesis in MS-1 [*Noguchi et al.*, 1999]. The majority of ferrous iron is presumed to be associated with the cell wall [*Ofer et al.*, 1984], where it becomes re-oxidized to low-density 2-line

ferrihydrite. The ferrous iron may be re-oxidized by coupling to either denitrification [*Yamazaki et al.*, 1995] or aerobic respiration [*Guerin and Blakemore*, 1992]. Magnetotaxis would be an advantageous trait for navigating across environmental redox gradients to facilitate such redox cycling of iron for metabolic purposes. Note that the purity of BCMM magnetite may be a result of this redox processing. The ORFs associated with the above processes include a highly similar (38–85%), but not conserved *nap*-type nitrate reductase (contig 3771 in MS-1, 404 in MC-1), two other nitroreductase family ORFs, and two hydrogenases.

1.1.3.3.2 Magnetite synthesis

After redox processing the ferrihydrite is transported to the magnetosome, not by a ferritin storage protein[*Vali and Kirschvink*, 1991], but by an unknown mechanism, perhaps by a conserved TolC-like transport complex. Once the low-density phase is in the magnetosome it is partially dehydrated to form a higher-density, crystalline ferrihydrite, and then converted to magnetite. All three phases have been observed within the magnetosome in MS-1 [*Frankel et al.*, 1983; *Mann et al.*, 1984]. The conversion to magnetite is thought to occur due to a ferrous iron ion bonding with the crystalline ferrihydrite, which then collapses into a soluble intermediate. This intermediate is further dehydrated and crystallizes as magnetite. Such conversions can spontaneously occur given proper pH, Eh, and ionic conditions [*Abe et al.*, 1999; *Mann et al.*, 1990] which could be regulated by the numerous conserved permeases and transporters. Magnetite may thus be synthesized through carefully regulated transport of the amorphous phase and ferrous iron ions to the magnetosome.

The control of crystal shape during magnetite synthesis appears to be carried out by matrices of modified proteins. Glycoprotein matrices have been implicated in morphological control in biomineralization in a variety of systems where the matrices are thought to provide nucleation sites and constraints on crystal growth by binding to the crystal itself (matrix-vesicle type biomineralization) [*Boskey*, 1998]. Conserved ORFs encode glycosyltransferases, sugar epimerases, and D-alanine exporters, all of which are members of glycoprotein synthesis and cross-linking pathways. The conserved *mms6, mamC,* and *mamD* ORFs have been shown to be tightly associated with the magnetite crystals within the magnetosome [*Arakaki et al.*, 2003]. Further, *mms6* has been shown to control crystal shape in magnetite precipitation experiments [*Arakaki et al.*, 2003]. The sequence similarity of these three ORFs with fibroin is very interesting as glycoprotein/fibroin matrices are a major component of other biomineralization systems [*Levi-Kalisman et al.*, 2001; *Pereira-Mouries et al.*, 2002].

The magnetosomes exist as chains in MS-1 and MC-1 and therefore must have some structure for maintaining the chain orientation of the magnetite crystals, as otherwise the chains would collapse upon themselves into a lower energy state [*Kirschvink*, 1982]. The *mam* cluster contains a conserved *mreB* -like gene (actin-homolog, contig 3824 ORF 4 in MS-1, ORF 619 in MC-1) which may be used for supporting magnetosome chains. This has been demonstrated in AMB-1 [*Komeili et al.*, 2006].

1.1.3.3.3. Regulation of BCMM

Some aspects of BCMM are not unique to BCMM (e.g., iron uptake, vesicle formation, and chemotaxis) and would not be expected to be conserved but would be expected to have conserved regulatory systems (If they are distinct from other regulatory systems). Approximately one fifth of the conserved ORFs are associated with chemotactic and cyclic nucleotide mono-phosphate signal transduction mechanisms, common methods for regulation of choice of metabolic pathways and response to external chemical signals. The conserved signal transduction elements include *cheB, cheR, cheW,* and *cheY* elements, as well as several histidine kinases and methyl-accepting chemotaxis proteins. There are also conserved elements of a cAMP signaling pathway, including adenyl cyclases and phosphodiesterases. These conserved signaling ORFs may also be used for regulation of conditions within the magnetosome and/or of choice of position in the environmental redox gradient appropriate to their energy needs.

1.1.3.4 Qualifications

It is important to note that not all ORFs involved in BCMM would be expected to turn up in our analysis. The aspect of a protein that makes it specific to BCMM may be of such short sequence length that other variations in sequence would hide the short conserved signal. Also some ORFs may not be specific to BCMM and are used for other functions which MS-1 and MC-1 share with other bacteria such that the ORFs do not appear conserved. Most importantly one must not make too much of the absence of ORFs from one or both genomes until the final assembly is complete, as rearrangements and gap closure will likely reveal more ORFs. Another danger is that there are sequenced

organisms which are not currently known to carry out BCMM but actually do, which would mask out ORFs important to BCMM. There is recent evidence that a close relative of the sequenced *Shewanella oneidensis*, *S. putrefaciens*, creates intracellular, membrane-bounded iron oxides [*Glasauer et al.*, 2002]. Other qualifications to note are: (1) by only comparing protein sequences we may have missed important similarities at the nucleotide level, such as promoter regions or ORFs not identified during draft analysis, and (2) protein function similarity and sequence similarity are not always correlated.

1.1.4. Conclusions

- We have identified a large set of conserved ORFs which fit into previous BCMM models.
- The presence and nature of the conserved ORFs indicates that MS-1 and MC-1 are using largely similar genetic mechanisms for BCMM and magnetotaxis.
- The finding of conserved metabolic ORFs lends support to the idea that BCMM is not just for navigational purposes but is also a metabolic strategy.
- These metabolic ORFs also lend support to evolutionary speculations where BCMM arose first as a metabolic strategy and was later exapted for navigation.

The conserved ORFs and the model developed will hopefully provide a useful framework for further elucidation of the mechanisms and evolution of BCMM. These ORFs prompt specific computational, genetic, and biochemical experiments which could accelerate the pace of discovery of BCMM mechanisms. It will be interesting to see if other BCMM organisms with different cellular structures and/or different habitats use similar genetic machinery.

Chapter One: Genomics

1.2. Targeted interruptions of genomically predicted genes

1.2.1. Introduction

To test the predictions generated by the comparison of the MS-1 and MC-1 genomes I undertook targeted interruptions of three conserved operons to see if this affected the phenotype. By inserting a drug resistance marker into the first gene of the operon I hoped to disrupt the synthesis of magnetite. Below are descriptions of the three operons selected for targeted interruptions.

Chemotaxis Pathway

There is a cluster of seven conserved genes in both MS-1 and MC-1 which encodes many components of a chemotaxis pathway (see Figure 2). Chemotaxis pathways are a means by which bacteria seek their optimal growth conditions, and the conservation of this chemotaxis pathway may be the result of similar growth requirements for MS-1 and MC-1. This seems unlikely as there are many other alpha-proteobacterial genomes sequenced which are phylogenetically between MS-1 and MC-1 and from organisms which share similar metabolic drives (e.g., microaerophily). Chemotaxis pathways are able to convey temporal information for transcriptional regulation and are able to interact with other protein complexes besides the flagellar motor. As such this chemotaxis pathway may be a mechanism for regulating the state of the magnetosome (e.g., redox poise or ionic concentrations). Another possibility is that

this conserved gene cluster is part of the hypothesized magnetosome battery, which would explain the unique metabolic requirements conserved only among MB.

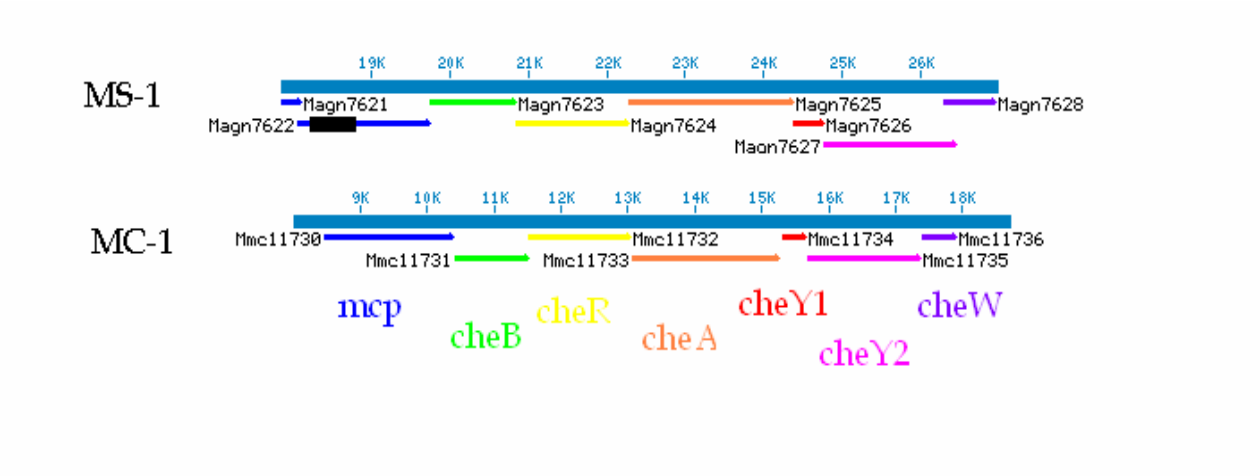

Figure 2: Chemotaxis gene cluster. Targeted interruption site is marked with the black box.

TolC Transporter Complex

This cluster (see Figure 3) encodes subunits of a TolC transport complex. This complex is normally used for the export of toxins and is also a channel through which phages are known to enter bacteria. The TolC complex spans both the outer and cytoplasmic membranes, and so is a direct channel to the cytoplasmic space. The conserved TolC complex in magnetotactic bacteria might function as a transport pathway across the cytoplasmic and magnetosome membranes to facilitate iron transport.

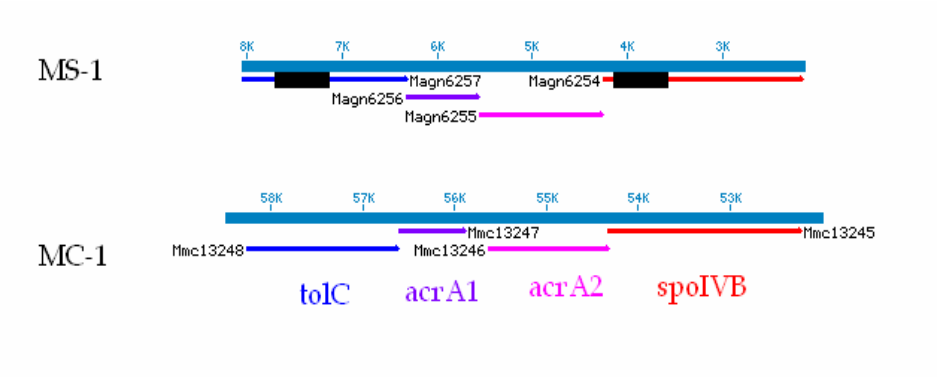

Figure 3: Cluster encoding predicted TolC transport complex. Targeted Interruption sites are marked with black boxes.

Hydrogenases 1 and 2

Large and small subunits of Hydrogenases 1 and 2 are conserved between MS-1 and MC-1 (See Figure 4). Hydrogenase 1 (HyaA and HyaB) is used by other bacteria for H_2 uptake, and Hydrogenase 2 (HybA and HybB) generates H_2 during fermentation of formate [*Maness and Weaver*, 2001]. It is not yet clear whether MS-1 or MC-1 are capable of hydrogen metabolism. It has been shown that there are several substrate-specific metabolisms (iron, nitrate, oxygen) which affect magnetite production, and it may be that hydrogen is another one.

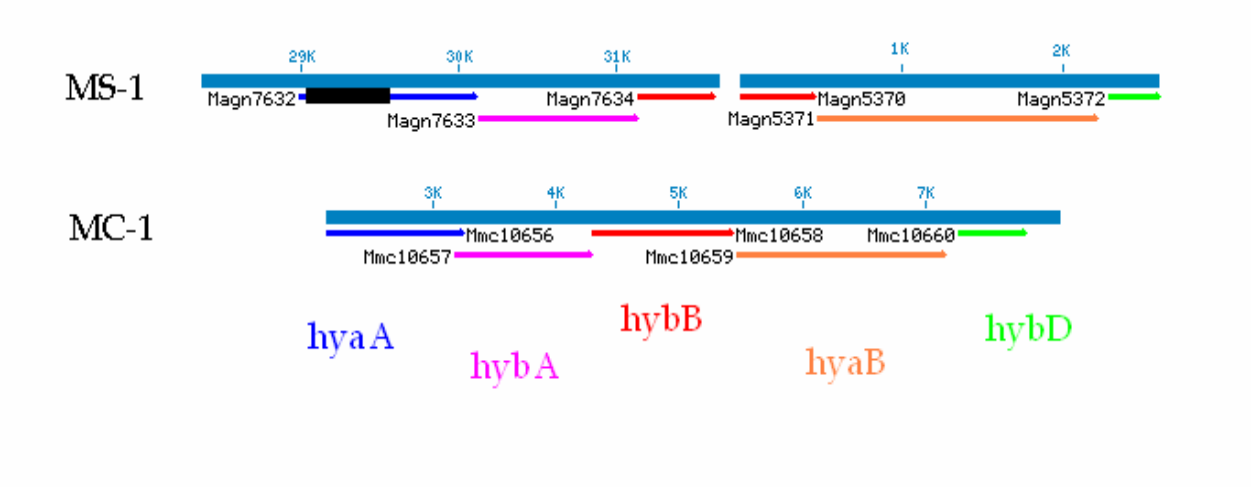

Figure 4: Conserved hydrogenase gene cluster. Targeted interruption site is marked with the black box.

1.2.2. Methods

Construction of Targeted Insertion Strains

Approximately 500 bp of the target gene was PCR amplified from AMB-1 DNA, purified and cloned into the TOPO vector (QIAGEN, USA). The target sequence was digested out of the TOPO vector with SpeI and NotI, purified, and ligated into the pAK31 vector. This plasmid was cloned into *E. coli* DH5α and transformed into donor strain *E. coli* wm3064. The donor strain was then mated with AMB-1 and transconjugants were selected for with kanamycin. Proper insertion was checked by PCR using a forward primer for the start of the interrupted gene and reverse primer reading out of the insertion.

Magnetization Assay

For the magnetization assay, stocks stored at -80˚ C were used to inoculate 1.5 ml of AMB-1 media without added iron in Eppendorf tubes and incubated at 30˚ C. After three days (late log phase) these cultures were added to 13.5 ml of AMB-1 medium

without added iron and allowed to grow overnight. The culture was centrifuged and resuspended in 1.5 ml of the original supernatant. 0.35 ml of the concentrated culture was then added to 10 ml of N_2 flushed AMB-1 media in Balsch tubes. Then 10 mM ferric quinate and air were added to achieve the specific test conditions. Cultures were then incubated at 30˚ C with shaking. Magnetization of the TI strains was checked by Cmag, the ratio of absorbance at 400 nm of cells aligned by external magnet parallel and perpendicular to the line of sight in the spectrometer.

1.2.3. Results and Discussion

None of the targeted interruptions caused a change in phenotype. Time course assays were carried out under varying iron and oxygen concentrations with no significant difference being found in magnetization (see Figure 5, 6, 7). This may be due to redundancy in the pathways in which these genes are involved; selection for genetic adaptation in the case of lethality of the TIs, the lack of their necessity for BCMM in our laboratory conditions, or these genes may not be involved in BCMM at all. If the genes are not involved in BCMM it raises the question why these genes are so well conserved among the magnetotactic bacteria. Since the targeted interruptions were undertaken, the hydrogenase genes have been found in new, non-BCMM genomes, further indicating that they are not necessary for BCMM. This demonstrates the necessity of testing of genomically generated hypotheses.

A more recent comparison using four MB genomes and 426 non-MB genomes found only 28 genes conserved among the MB [*Richter et al.*, 2007]. This analysis used the complete genomes of MC-1 and *Magnetospirillum magneticum* AMB-

1, and the draft genomes of MS-1 and *M. gryphiswaldense* MSR-1. Richter et al. found 15 of the *mam* genes conserved as well as 13 genes outside of the *mam* cluster. We found 13 of their 15 *mam* genes conserved in our study — we did not find the short proteins *mamQ* or *mamC* conserved. We only found 7 of the 13 genes they found outside of the *mam* cluster. This includes *mtxA, mmsF,* and *mamX* as well as two predicted hemerythrins, a *mamH*-like gene, and a phage.

There are a number of differences in the methods that could account for the different set of genes found between this study and Richter et al.'s 2007 study. First, they used expectation values to compare BLAST hits. Expectation values are based in part on the size of the database used for searching, and thus will change from one search to the next. Our use of bit scores, which aren't tied to database size, facilitate consistent comparisons. Ideally one would use an alignment and scoring algorithm with a rigorous statistical base, such as HMMER (http://hmmer.wustl.edu). The second, and perhaps greatest difference, is the way they searched the non-magnetotactic genomes. They restricted their conserved genes (their "MTB-related genes") to not having a BLAST hit outside of the MB with an E-value less than 1e-50. This eliminates many of the proteins identified in our study as they were found to have significant similarity to proteins outside of the MB, though not as high a similarity to other MB proteins. When they included significant hits (i.e., E-value < 1e-80) to *Rhodospirillum rubrum*, the phylogenetically closest non-MB genome to the magnetospirilla, they found only one gene conserved. Finally, their use of twice as many MB genomes and non-MB genomes in their analysis likely eliminated some of the genes we identified in our more limited analysis.

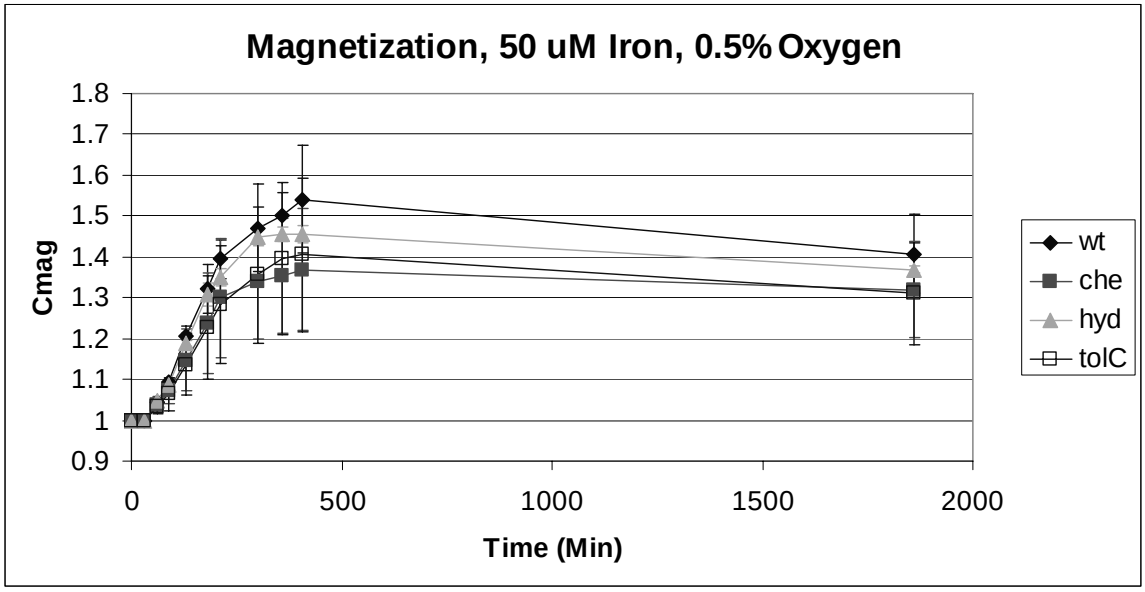

Figure 5: Time course of acquisition of magnetization by TI strains (che: Chemotaxis cluster, hyd: Hydrogenase cluster, tolC: TolC cluster) versus wild-type (wt). High iron concentration and low oxygen allowed the cultures to become very magnetic. Error bars are the average of 3 subcultures of a culture passaged under the same conditions.

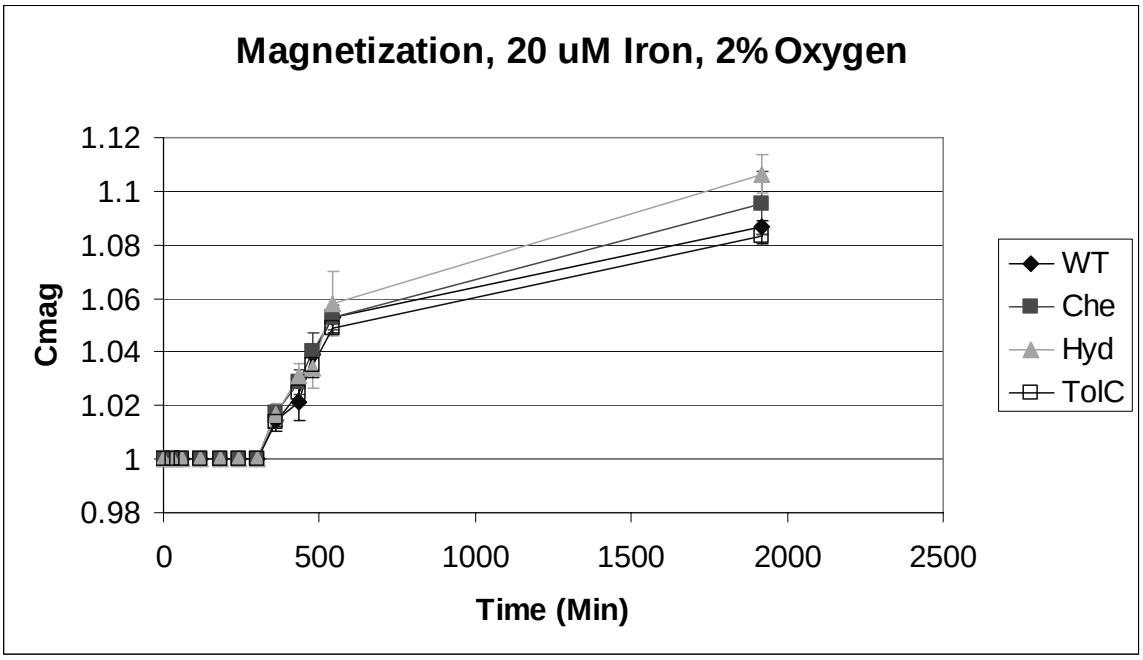

Figure 6: Time course of acquisition of magnetization by TI strains (che: Chemotaxis cluster, hyd: Hydrogenase cluster, tolC: TolC cluster) versus wild-type (wt). Lower iron and higher oxygen reduced the total magnetization acquired and delayed the onset of magnetization. Error bars are the average of 3 subcultures of a culture passaged under the same conditions.

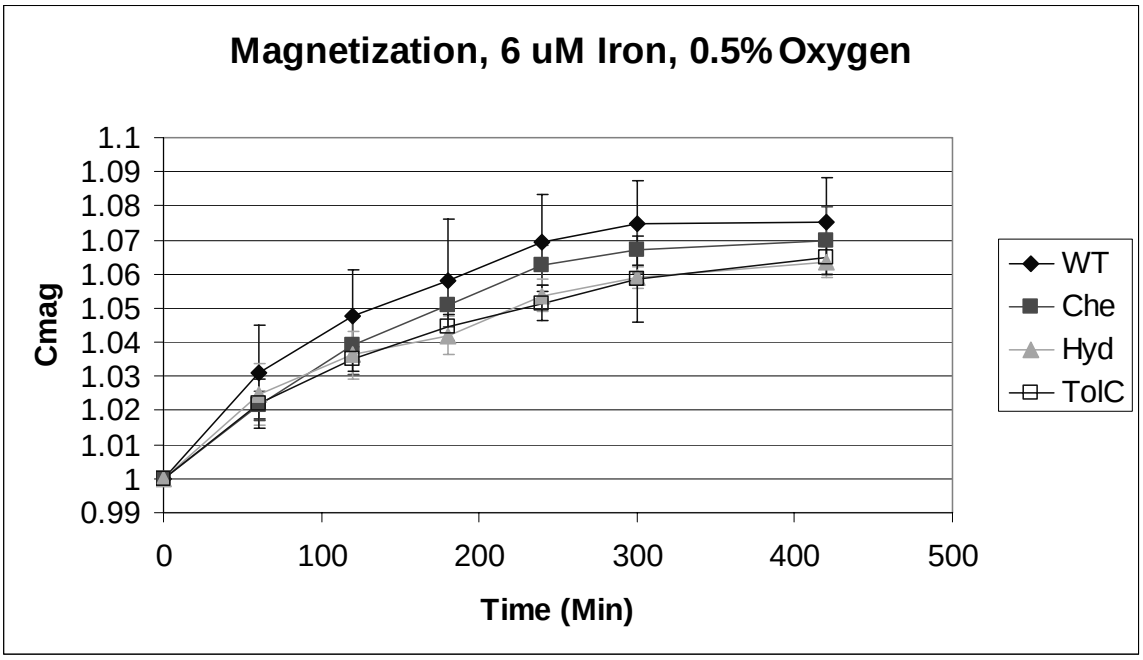

Figure 7: Time course of acquisition of magnetization by TI strains (che: Chemotaxis cluster, hyd: Hydrogenase cluster, tolC: TolC cluster) versus wild-type (wt). Very low iron and low oxygen reduced the total magnetization acquired without delaying the onset of magnetization. Error bars are the average of 3 subcultures of a culture passaged under the same conditions.

Chapter Two: Genetics

2. Transposon Mutagenesis Analysis of Magnetotactic Biomineralization

Cody Z. Nash, Arash Komeili, Robert E. Kopp, Atsuko Kobayashi, Hojatollah Vali, Dianne K. Newman, and Joseph L. Kirschvink

2.1. Introduction

Magnetotactic bacteria (MB) are distinguished from other bacteria by their ability to synthesize intracellular magnetic crystals in the single-domain size range. In laboratory strains of MB the crystals are mainly composed of the iron oxide magnetite (Fe_3O_4) with minor amounts of other iron oxides. These crystals occur within lipid-membrane-bounded spaces termed magnetosomes, which have a distinct population of proteins from that of the other cell membranes. These crystals are generally chemically pure, have no crystallographic defects, and are arranged into chains. Different strains of magnetotactic bacteria form different shapes of crystals, and some strains produce the magnetic iron sulfide Greigite. Within each strain the shape and composition of crystals is uniform, which suggests that there is genetic control over their synthesis.

A number of studies have identified the genes involved by using transposon mutagenesis. In this technique bacteria are mutated by introducing a transposon to them through conjugation with a donor strain. The transposon carries a drug resistance marker which allows the transconjugants to be isolated. The resulting population can then be screened in various ways to isolate mutants in a specific phenotype. The gene responsible can then be discovered by determining the insertion site of the transposon.

Previous studies have demonstrated the role of several genes necessary for the magnetotactic phenotype, including iron transporters, flagellum, and regulatory genes.

In this study we screened through 5809 mutants to identify more of the genes involved in the process. Nineteen non-magnetic or partially magnetic mutants were identified. Fourteen of these were in the *mam* cluster, an island of genes which encode many of the proteins found in abundance in the magnetosome membrane. The other five mutants have insertions in genes outside of the *mam* cluster. The necessity of genetic machinery outside of the *mam* cluster indicates that magnetotaxis may not be as easily laterally transferred as has been previously speculated. It also suggests a number of previously unsuspected pathways may be involved in the magnetotactic phenotype.

2.2. Methods

Mutagenesis

To generate mutants, the Mariner transposon was introduced to *Magnetospirillum magneticum* AMB-1 through conjugation with a donor strain, *Escherichia coli* β2155, as previously described [*Komeili et al.*, 2004]. Selection was done with Kanamycin at 5 μg/ml. Transconjugation rates of up to 5e-05 were achieved. Timing was critical to prevent spontaneous mutants.

Magnetic Screen

Mutants were screened by growing them in 96-well plates and, after grown, placing them over an array of magnets, as previously described [*Komeili et al.*, 2004]. Magnetic mutants were pulled to the sides of the wells, while non-magnetic mutants remained at the bottom (See Figure 1).

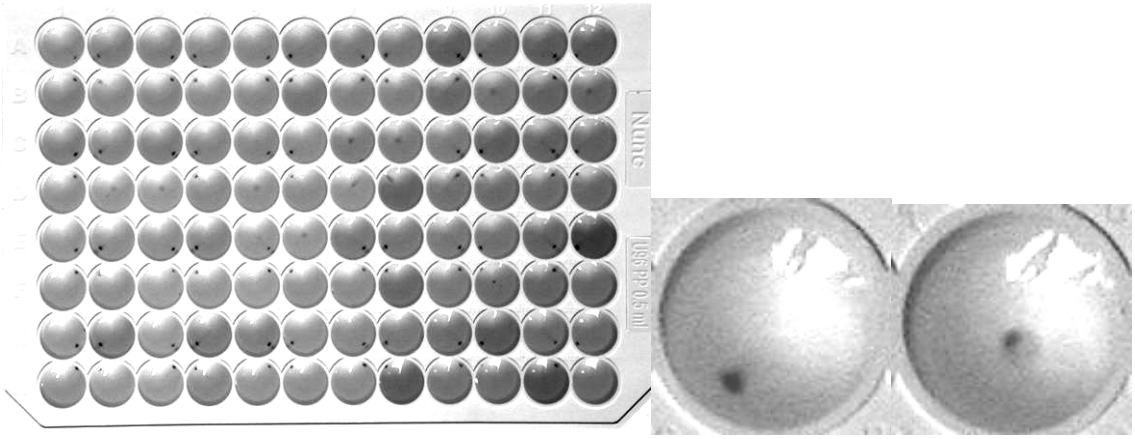

Figure 1: Magnetic screen for non-magnetic mutants. (a) A plate of transconjugants placed over an array of magnets to pull the MB to the side of the wells. (b) Close-up of a magnetic and non-magnetic mutant

PCR Screen

Due to the high rate of spontaneous mutation in strain AMB-1, non-magnetic mutants were checked for deletions in the *mam* cluster. Mutants were initially screened for the presence of *mamA*, and then along 16 kb of the *mam* cluster. PCR was used to amplify 1–3 kb sections of the *mam* cluster to determine their presence, absence, or change in length. Amplifications were carried out with Promega 2X PCR mix (Promega Corporation, Madison, WI, USA) with 30 cycles and a 56˚ C annealing temperature.

List of Primers for PCR screen:

MamA-up	5' GGCGAATTCATGTCTAGCAAGCCGTCGGA 3'
MamA-down	5' GGCGGATCCGACCGAGGCCCCTTCGTCAAGT 3'
ClBeg	5' GTTCAGGTCGGTGGGTTTTT 3'
ORF2-2	5' GTTCGGCAAGACCGAAATTA 3'
ORF2-1	5' GCGTGGAAGAGGTCGAGA 3'
ORF5-2	5' CTTGTATCTCCGGCTTCTCG 3'
ORF5-1	5' CGTCAATGTGGCCATGTATT 3'
ORF7d	5' ACATTGCCCTTGACCACATT 3'
ORF7c	5' CGAGAAGTTCCTGCATTTCC 3'
AQ2	5' ACGGCCAGATCGTACTTTTG 3'
AQ1	5' GGGAATCGCCTATGTGAAGA 3'
ORF11-2	5' GCGACAGATTTTCCAAAACG 3'
ORF11-1	5' ACGTCAAGTCGATCCAGGTC 3'
ClEnd	5' CTCGCAAACACTCAAGACACTCAG 3'

Magnetization Measurements

For time-course experiments, magnetization was measured by absorbance at 400 nm wavelength. Magnetic cultures have a higher absorbance when they are aligned parallel to the line of sight than when aligned perpendicularly. Alignment was induced by placing a large stir bar magnet adjacent to the culture during measurement. The ratio of parallel to perpendicular absorbance is defined as Cmag.

For moment per cell measurements, 1600 mT isothermal remnant magnetization was measured on 1.5 ml cultures in Eppendorf tubes with a 2G Enterprises SQUID magnetometer. Culture density was determined by direct cell counts.

TEM Imaging

Conventional TEM and HAADF/STEM/EDX analysis was carried out on a Tecnai G2 F20 Twin (FEI, Holland), as described previously [*Kobayashi et al.*, 2006]. Cryo-TEM was carried out with a JEOL JEM-2000FX TEM as previously described [*Komeili et al.*, 2004].

Complementation

The pAK4 vector, a modified pBBR1MCS4 vector containing a *tac* promoter, was used as the base for complementation plasmids. Sequences to be complemented were PCR amplified with the high fidelity polymerase EHF (Roche, Switzerland), ligated into the pAK4 backbone, cloned into DH5α λpir, transformed into donor strain wm3064, and then into the mutant strain. Selection was done with Ampicillin or Carbenicillin.

Targeted Interruption

The pWM91 vector was used as the base for targeted interruptions [*Metcalf et al.*, 1996]. 1 kb target sites were amplified with ThermoPol polymerase (NEB, USA), ligated into the pWM91 backbone, cloned into DH5α λpir, transformed into donor strain wm3064, and then inserted into the chromosome of wild-type *Magnetospirillum*

magneticum AMB-1 via homologous recombination. Selection was done with Kanamycin.

Strains and Plasmids Used:

Magnetospirillum magneticum AMB-1 [*Matsunaga et al.*, 1991]

E. coli DH5a cloning strain for vector construction [*Sambrook et al.*, 1989]

E. coli wm3064 donor strain for mutagenesis [*Dehio and Meyer*, 1997]

E. coli b2155 for mutagenesis

PSC189 — hyperactive mariner transposon [*Chiang and Rubin*, 2002]

pAK [*Komeili et al.*, 2004]

2.3. Results and Discussion

Out of 5809 mutants screened, 192 were initially found to be non-magnetic. Most of these were found to be spontaneous mutants during the PCR screen. The rate of spontaneous mutation decreased from 11% to 0.5% when care was taken to minimize the amount of time in stationary phase the AMB-1 cultures experienced prior to mating. This is consistent with previous work showing a correlation between time in stationary phase and spontaneous mutation in MB, probably due to native transposon activity [*Schübbe et al.*, 2003; *Ullrich et al.*, 2005]. 19 of the 192 were found to be non- or partially magnetic and not due to deletions of all or part of the *mamAB* cluster based on the PCR assay. Of the 19 non-magnetic mutants, 14 had insertion sites inside the *mamAB* cluster in six different genes (see Figure 2). The five mutants with insertion sites outside of the *mamAB* cluster are discussed individually below.

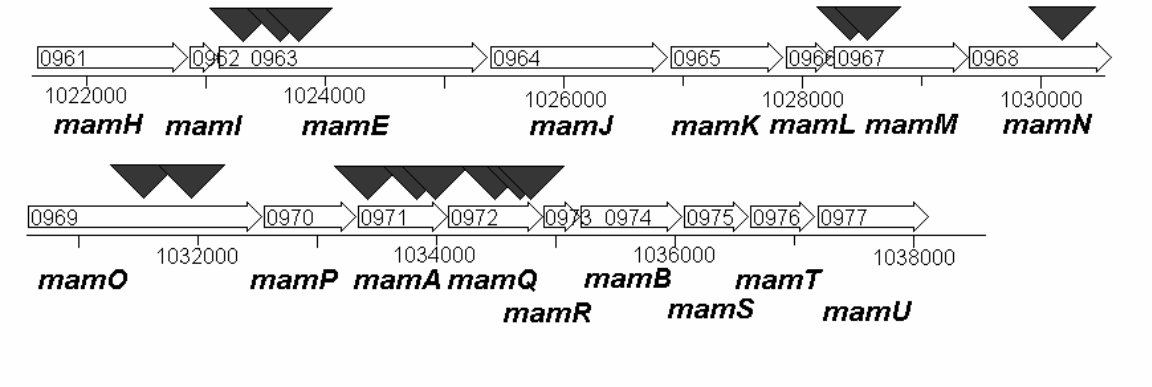

Figure 2: Map of insertion sites in the *mamAB* cluster in AMB-1. Locus numbers are inside the genes, map position below the scale, gene names below the scale, and insertion sites are marked with the arrowheads.

MNM9

Mutant MNM9 has a transposon insertion site 99088 base pairs from the origin of the chromosome, near the beginning of predicted gene amb0089. Magnetic measurements show that it is completely non-magnetic. HAADF TEM showed an absence of magnetite (See Figure 3a). Cryo-TEM also shows an absence of magnetite, but further shows that MNM9 lacks magnetosomes entirely, membranes and all (See Figure 3b & 3c).

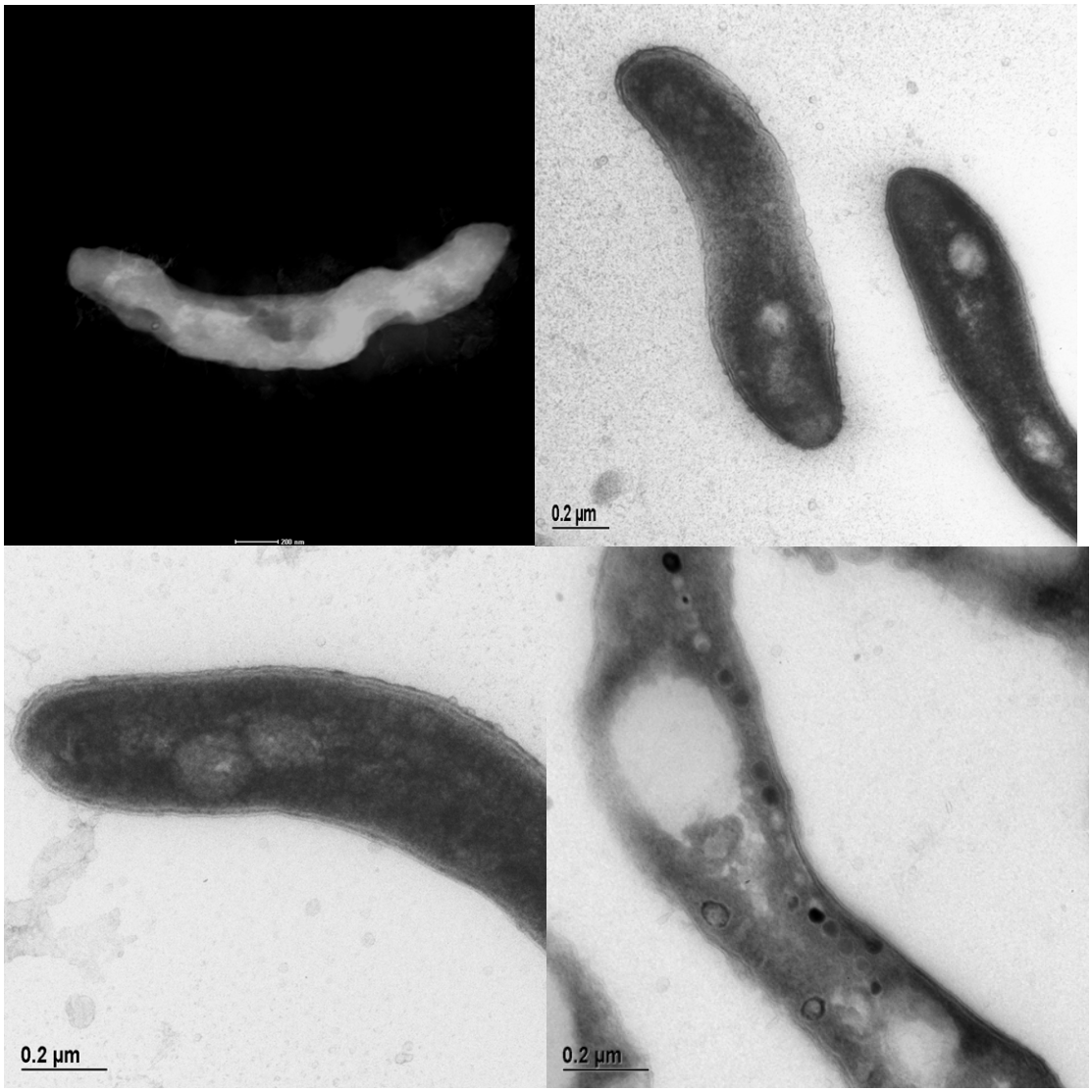

Figure 3: (a) HAADF TEM of MNM9 showing absence of inclusions. (b) and (c) Cryo-TEM of MNM9 showing complete absence of magnetosomes. (d) Cryo-TEM of wild-type AMB-1 for comparison

Complementation of MNM9 with amb0089; amb0089 and amb0090; or amb0089, amb0090, and amb0091 failed to recover any of the wild-type phenotype. Targeted interruption of amb0089 failed to alter the wild-type phenotype. This suggests that

MNM9's phenotype may be due to a spontaneous mutation in some other part of the chromosome, although large-scale deletions in the *mamAB* cluster were ruled out by the PCR screen. The discovery and development of efficient native promoters in AMB-1 may allow better complementation in the future [*Yoshino and Matsunaga*, 2005]. The failure of the targeted interruption to replicate the MNM9 phenotype may be because the interruption did not replicate necessary polar effects.

The predicted gene amb0089 is a predicted Fe-S oxidoreductase and falls into the Radical SAM protein superfamily. These proteins have an iron-sulfur center which generates organic radicals from the S-adenosylmethionine (SAM) molecule (for reviews, see [*Fontecave et al.*, 2004; *Layer et al.*, 2004]). Radical SAM proteins can act in a regulatory role by catalyzing the methylation of DNA, hormones, neurotransmitters, and signal transduction systems. They also play a role in numerous biosynthetic pathways by catalyzing the addition of parts of the SAM molecule to the substrate. Many of the predicted genes near amb0089 which code in the same direction belong to the sialic acid biosynthesis pathway (See Figure 4). Sialic acid is a terminal sugar residue on glycoproteins which is expressed on the outer surface of membranes in eukaryotes to regulate vesicle transport. Sialic acid is also commonly used by pathogenic bacteria to evade an immune response. What sialic acid is doing in AMB-1 is still a mystery.

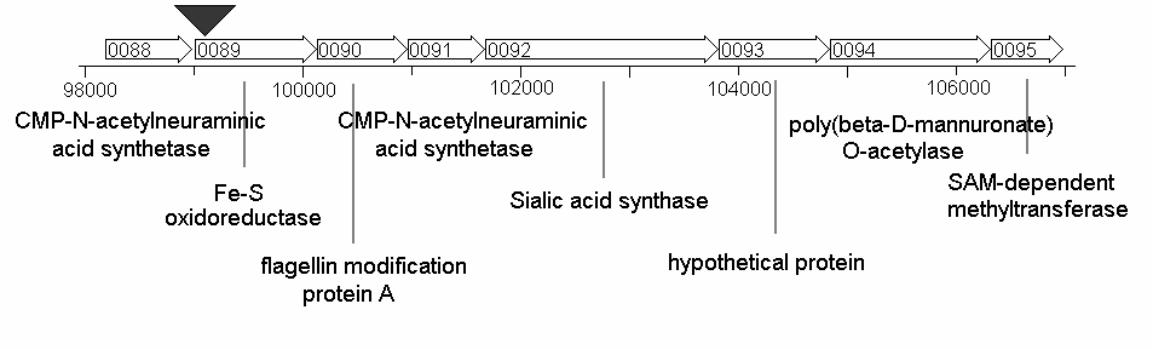

Figure 4: Location of transposon insertion for MNM9. Locus numbers are inside the genes, map position below the scale, predicted product below the scale, and the insertion site is marked with the arrowhead.

MNM13

Mutant MNM13 has an insertion site at 197516 bp along the AMB-1 chromosome, in the middle of gene amb0172. Magnetization assays showed it to have a weakly magnetic phenotype. Cryo-TEM shows MNM13 to have isolated, elongate crystals (See Figure 5) in contrast to the equant crystals produced by wild-type AMB-1.

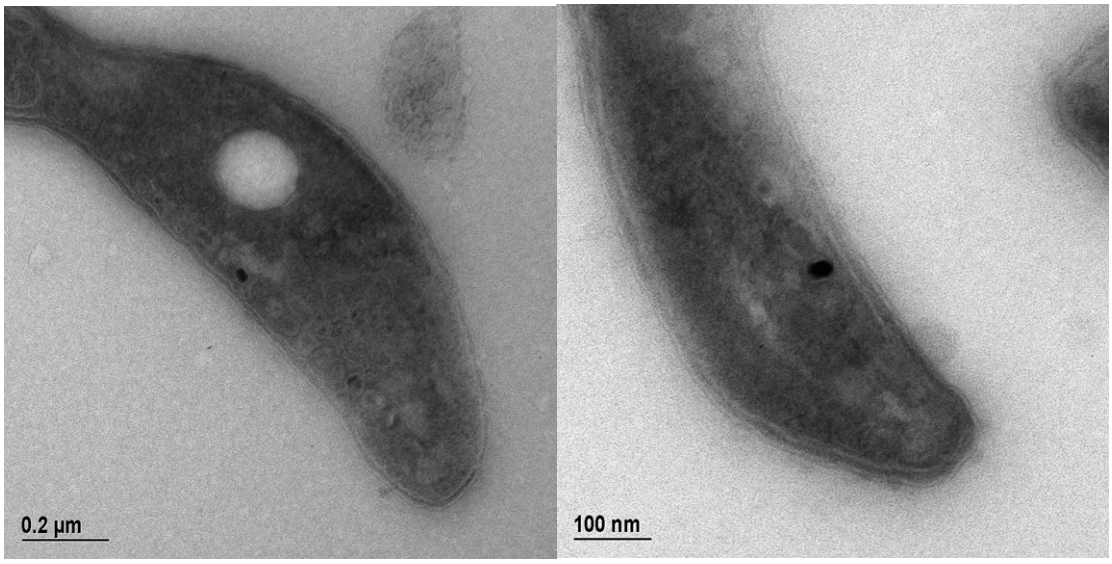

Figure 5: Cryo-TEM of MNM13 showing isolated, elongate crystals

Complementation of gene amb0172 or amb0172 and amb0173 failed to change the phenotype of MNM13. Gene amb0172 is a predicted hydrolase or acyltransferase, and the adjacent genes coding in the same direction are a hypothetical protein and a predicted aldehyde dehydrogenase (see Figure 6).

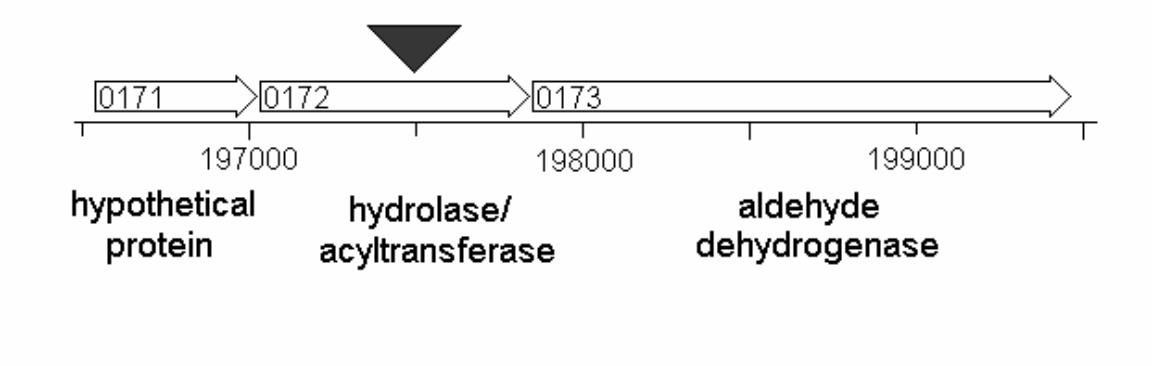

Figure 6: Transposon insertion site for MNM13. Locus numbers are inside the genes, map position below the scale, predicted product below the scale, and the insertion site is marked with the arrowhead.

MNM16

MNM16 has its transposon insertion site at 225328 bp along the AMB-1 chromosome near the end of predicted gene amb0200. Magnetization assays indicated it was partially magnetic (see Figure 7) and conventional TEM revealed fewer crystals scattered along the magnetosome chain, with each crystal appearing normal (see Figure 8).

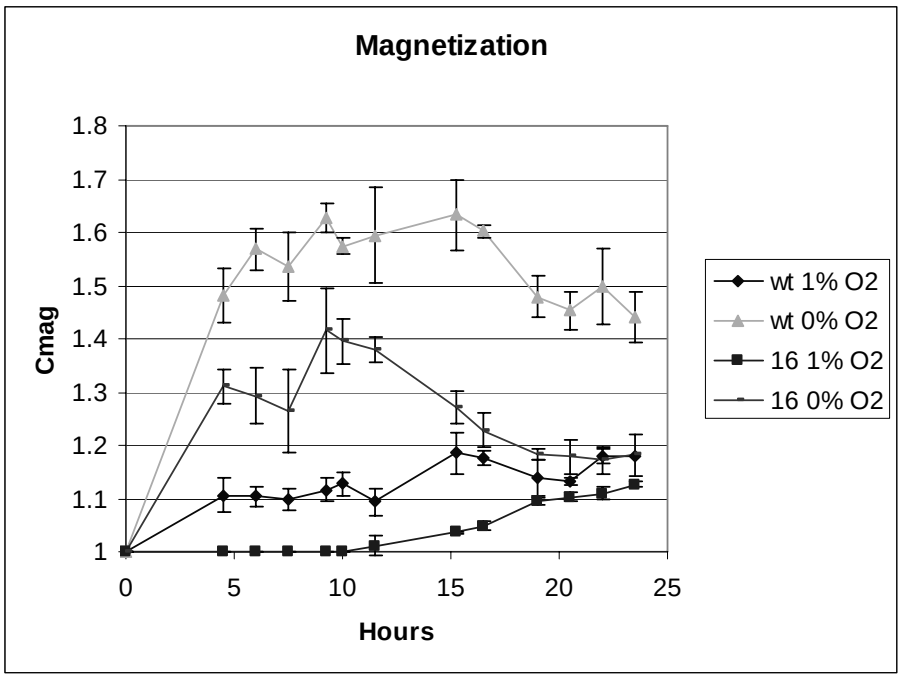

Figure 7: Magnetization assays of MNM16 under 0% and 1% O_2 in headspace, as compared to wild-type. Error bars are the average of 3 subcultures of a culture passaged under the same conditions.

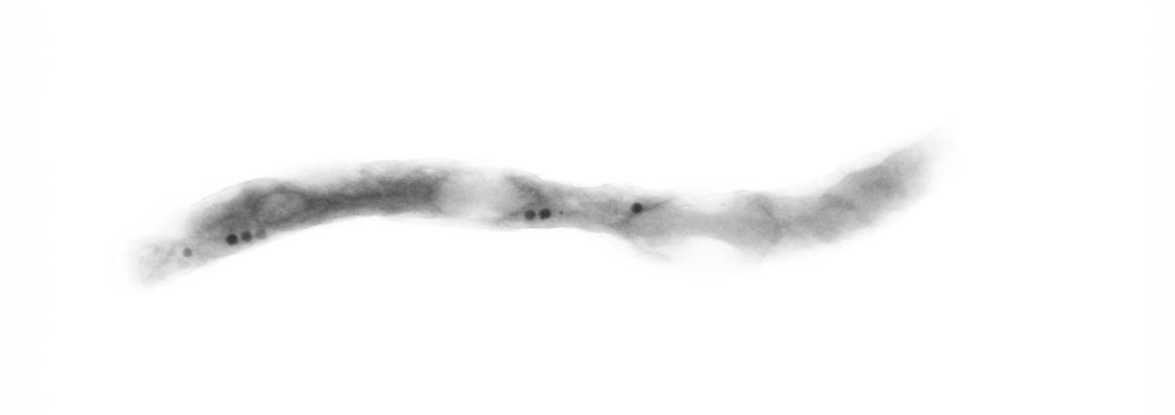

Figure 8: TEM of MNM16 showing fewer crystals than in wild type

Complementation of gene amb0200 did not have any significant effect on the phenotype, while complementation of genes amb0200 through amb0196 (on the

complementary strand) partially restored the phenotype both in Cmag and IRM measurements of magnetization (see Figures 9 and 10).

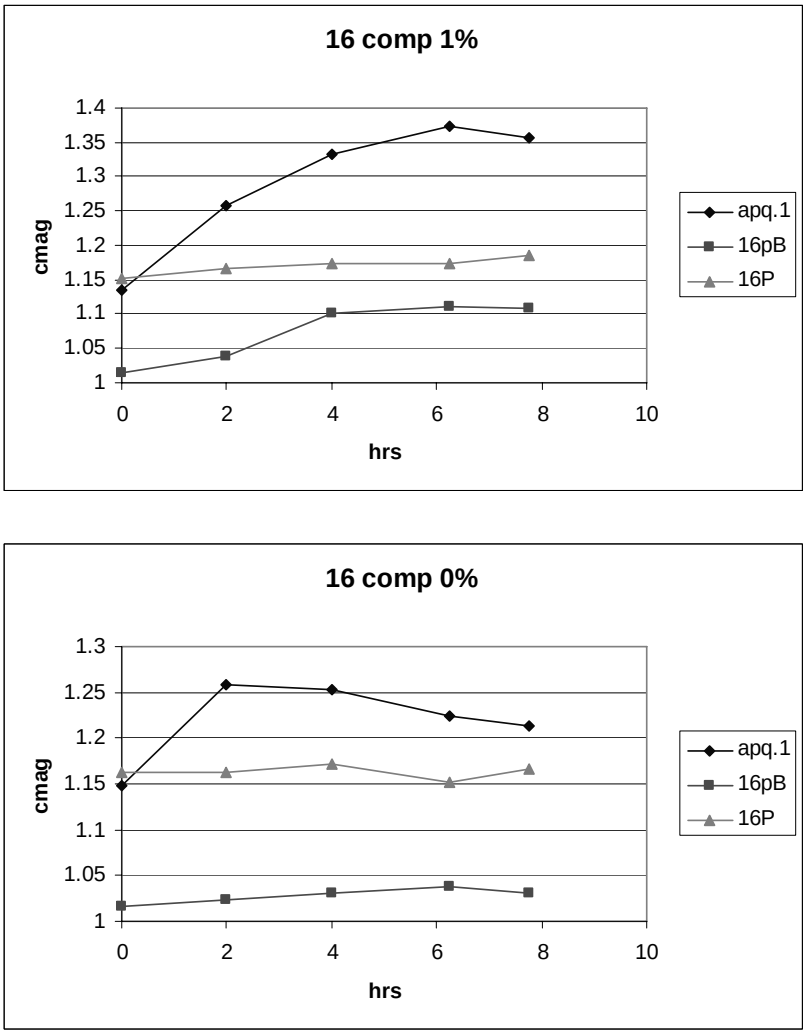

Figure 9: Time course of complementation of MNM16. (a) Experiments with 1% O_2 in headspace of Balsch tubes. (b) Experiments with 0% O_2 in headspace of Balsch tubes. 16pB is mutant mnm16 carrying an empty complementation vector to confer Ampicillin resistance. 16P is complemented for the mutated gene and downstream genes (see text for discussion). APQ.1 is wild-type AMB-1 carrying the Ampicillin and Kanamycin resistance carrying plasmid APQ.1. Growth curves are from single cultures.

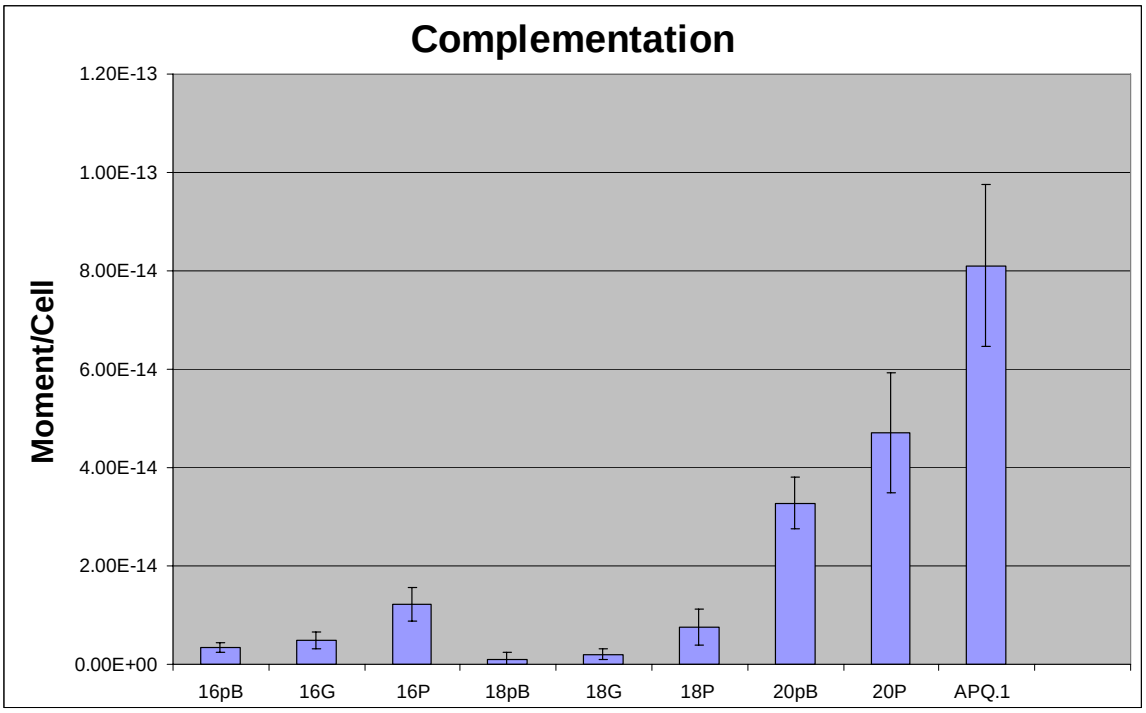

Figure 10: Complementation assays for MNM16, MNM18, and MNM20. 16pB, 18pB, and 20pB are mutants mnm16, 18, and 20 carrying an empty complementation vector to confer Ampicillin resistance. 16G and 18G are mnm16 and 18 with only the mutated gene complemented. 16P, 18P, and 20P are complemented for the mutated gene and downstream genes (see text for discussion). APQ.1 is wild-type AMB-1 carrying the Ampicillin and Kanamycin resistance carrying plasmid APQ.1. Error bars are the average of 3 subcultures of a culture passaged under the same conditions.

MNM16's insertion is in a predicted transcriptional regulator. Complementation of this gene alone did not significantly change the phenotype, while complementation of amb0200 and four of the downstream genes did have a significant effect. This suggests that one of the downstream genes is responsible for the phenotype. These genes are predicted to be of various and uncharacterized functions (see Figure 11), and in that way

resemble the genes of the *mamAB* cluster. This diversity of predicted function may be how a new pathway appears in annotation.

The reduced number of crystals seen in MNM16 is similar to that seen in AMB-1 when *mamA* is knocked out [*Komeili et al.*, 2004]. It would be very interesting to see if the expression of the *mam* genes is affected in the same manner in both MNM16 and *mamA* deletions.

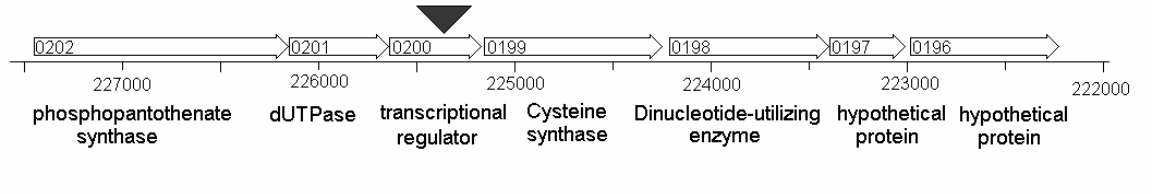

Figure 11: Transposon insertion site of MNM16 and nearby genes. Locus numbers are inside the genes, map position below the scale, predicted product below the scale, and the insertion site is marked with the arrowhead.

MNM18

The transposon insertion site of MNM18 is at base pair 3494968 in gene amb3233. MNM18 is partially magnetic (see Figure 12) and is the only mutant to display a growth defect. TEM shows that MNM18 produces 1–2 equant crystals per cell (See Figure 13).

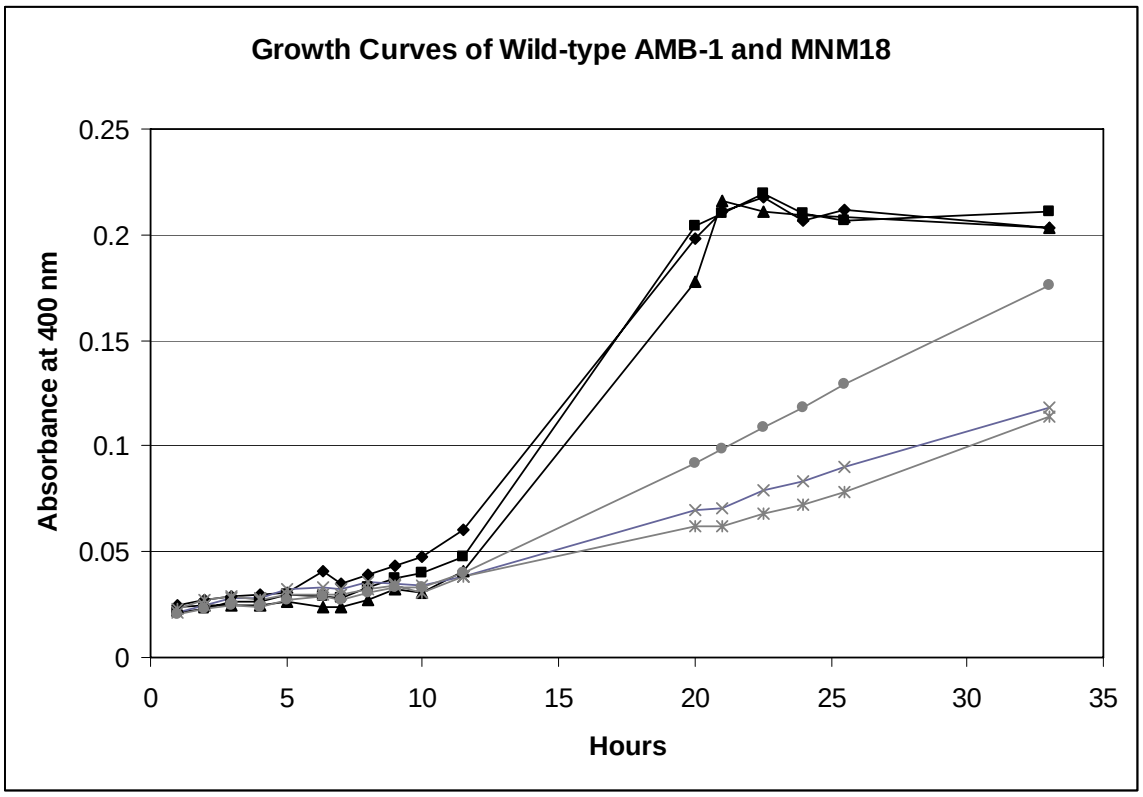

Figure 12: Growth curves of MNM18 versus wild-type. Wild-type is in black, MNM18 is in light grey. Curves are not averaged so that the individual behavior of each culture can be examined. The 3 wild-type and mnm18 cultures are subcultures of a single culture passaged under the same conditions as the experiment.

Figure 13: TEM of MNM18 showing one large equant crystal and one small, poorly formed crystal

Complementation of amb3233 alone did not have a significant effect, but complementation of genes amb3233, amb3234, and amb3235 significantly restored the phenotype in both time course Cmag and IRM magnetization assays (see Figures 10 & 14). The complementation did not restore the growth defect. This may be due to the low level of complementation achieved for the magnetization. Complementation of the growth defect may be too low to detect with this construct.

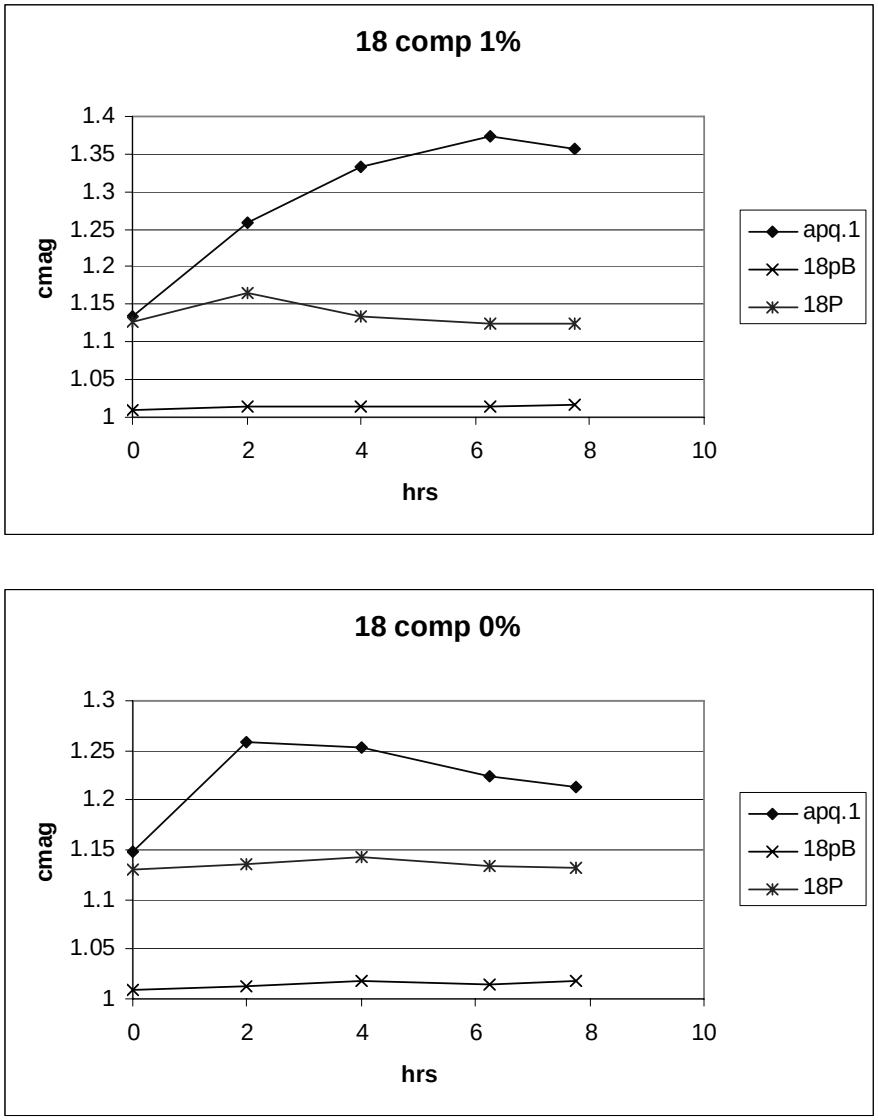

Figure 14: Time course of complementation of MNM18. (a) Experiments with 1% O_2 in headspace of Balsch tubes. (b) Experiments with 0% O_2 in headspace of Balsch tubes. 18pB is mutant mnm16 carrying an empty complementation vector to confer Ampicillin resistance. 18P is complemented for the mutated gene and downstream genes (see text for discussion). APQ.1 is wild-type AMB-1 carrying the Ampicillin and Kanamycin resistance carrying plasmid APQ.1. Growth curves are from single cultures.

The gene amb3233 is a predicted to encode the α and β subunits of a pyruvate/ferredoxin oxidoreductase. The downstream genes are the γ-subunit and a cheY gene, and the upstream gene is a predicted transcriptional regulator (see Figure 15). The genes flanking this cluster code on the opposite strand. The growth defect of MNM18 is consistent with a disruption of metabolic genes.

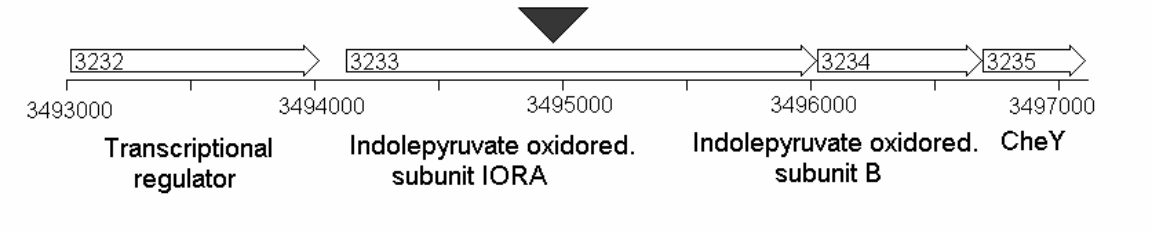

Figure 15: Insertion site of MNM18. Locus numbers are inside the genes, map position below the scale, predicted product below the scale, and the insertion site is marked with the arrowhead.

MNM20

MNM20 has its insertion site at position 553134, in gene amb0516. Magnetization assays show MNM20 to be partially magnetic and HAADF TEM shows that it has many poorly formed and amorphous crystals (see Figure 16).

MNM20 sometimes grows without any defect in magnetization, and it is not clear what growth conditions are necessary to produce the mutant phenotype. It is possible that the frequent spontaneous mutations AMB-1 experiences are able to revert MNM20 to the wild-type phenotype.

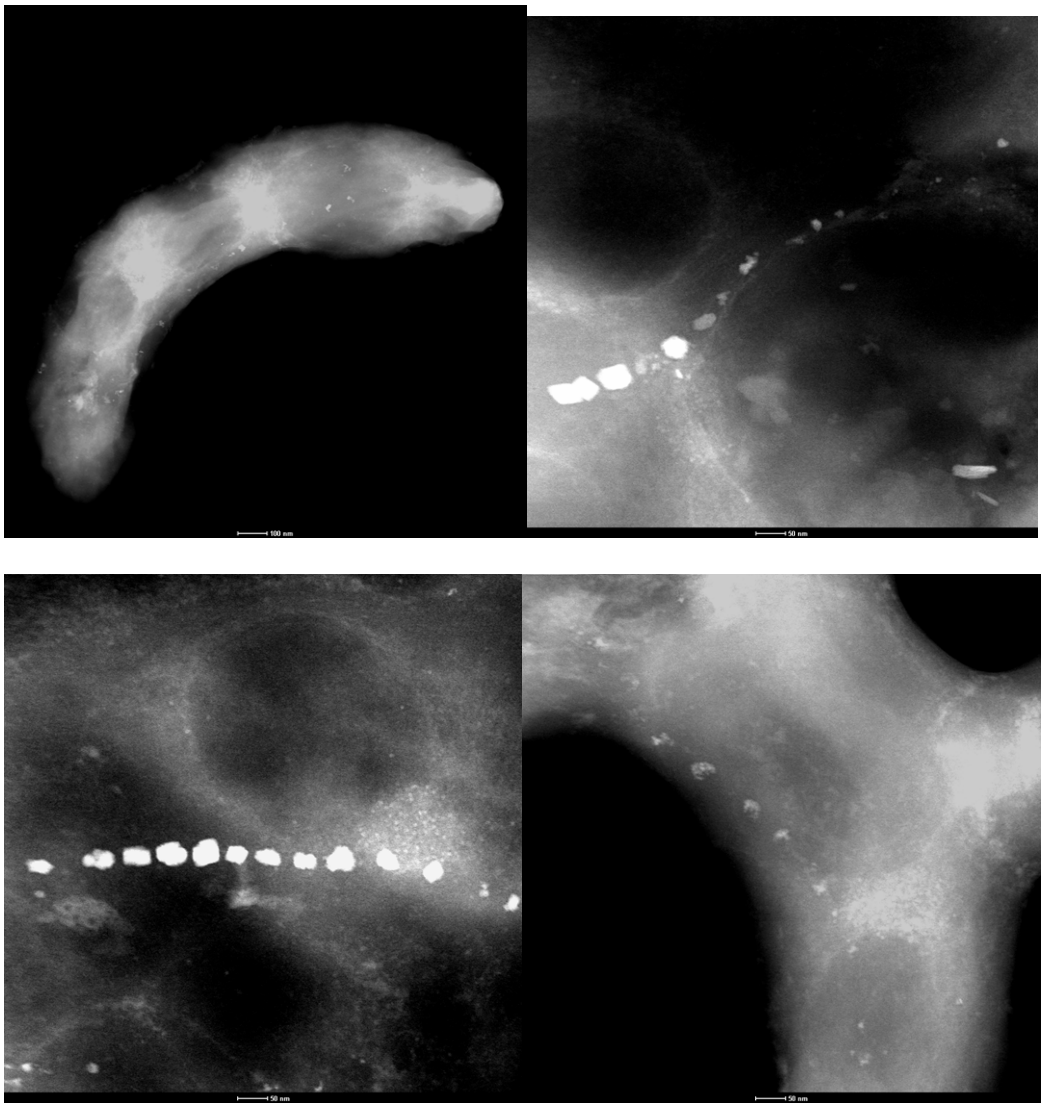

Figure 16: HAADF TEM images of MNM20 showing many poorly formed and amorphous crystals

The gene amb0516 is a hypothetical protein with few matches outside of the *Magnetospirilla*. The downstream gene amb0517 is even more unusual in that it is similar to many eukaryotic proteins. This gene cluster (see Figure 17) again displays the

trait of genes with various and poorly characterized functions, suggesting involvement in a poorly understood pathway.

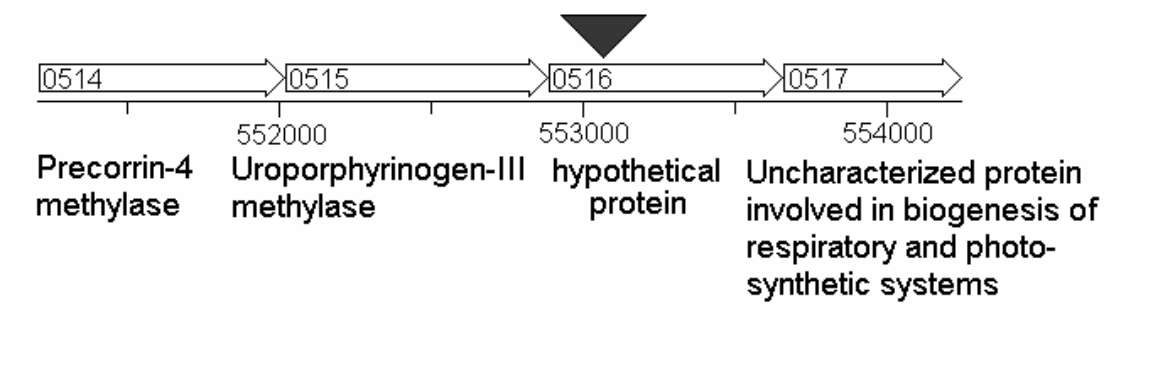

Figure 17: Insertion site of MNM20. Locus numbers are inside the genes, map position below the scale, predicted product below the scale, and the insertion site is marked with the arrowhead.

2.4. Conclusions

Out of 5809 mutants screened, 19 were identified as non- or partially magnetic and did not have large deletions in the *mamAB* cluster. Fourteen of these are insertions in the *mamAB* cluster, demonstrating its role in the magnetic phenotype of magnetotactic bacteria. Five mutants have insertions in genes outside the *mamAB* cluster, suggesting that the genetic systems necessary for the wild-type magnetic phenotype are not restricted to a few clusters of genes. The difference between the genes identified in this mutagenesis and others may be due to the different transposons used. In comparing this study with other transposon mutagenesis studies in magnetotactic bacteria, this is the only one to use a PCR screen, which may account for the lower total number of non-magnetic mutants seen (see Table 1).

The absence of insertions in the *mamGFDC* cluster, another cluster of genes which encode magnetosomal proteins, is consistent with recent results that these genes are not necessary for a magnetic phenotype [*Scheffel et al.*, 2008]. The absence of insertions in the *mamJ* and *mamK* genes is also consistent with recent work showing that these genes affect magnetosome localization but not magnetite formation in the magnetospirilla [*Komeili et al.*, 2006; *Scheffel et al.*, 2006].

There are a number of methods which future investigators could use to examine the role of these genes in magnetotaxis. One could test recently developed high-efficiency native promoters to try to improve the complementation of the mutants [*Yoshino and Matsunaga*, 2005]. Another route to conclusively testing the role of these genes would be to carry out knock outs of the genes, which would eliminate the possibility of read-through from the drug resistance marker inserted during targeted interruptions. Targeted interruptions can also generate incomplete versions of the protein they interrupt, either from the fragment before or after the insertion. These incomplete versions may retain full functionality in the conditions assayed or may interfere with other cellular processes to mask any effect on magnetite biomineralization. A knock out avoids these possibilities.

Finally, another way to examine these mutants is to look at the mRNA levels of the relevant genes. Through reverse transcriptase PCR (RT PCR) one could check the expression levels of *mam* genes to see which, if any of the mutants has altered regulation of these genes known to be involved in magnetotaxis. RT PCR would also allow one to determine how effective complementation is relative to the mutant expression levels of the mutated genes. It could also be used to compare expression levels of the *mam* genes

between mutants, targeted interruptions, and knock outs to see if the latter two methods are replicating the mutant phenotype at the RNA level.

Table 1: Transposon Mutagenesis Studies in Magnetotactic Bacteria

Strain	**Transposon**	**Mutants Screened**	**Non-magnetic**	**Insertion sites identified**	**Ref**
AMB-1	Mini-Tn5	118	5	amb3990 (magA)	[*Matsunaga et al.*, 1992; *Nakamura et al.*, 1995]
AMB-1	Mini-Tn5	5762	69	amb0192, amb0291, amb0503, amb0521, amb0676, amb0741, amb0759, amb1309, amb1394, amb1482, amb1692, amb1722, amb1790, amb2051, amb2087, amb2504, amb2554, amb2611, amb2660, amb2765, amb2922, amb3184, amb3268, amb3279, amb3295, amb3450, amb3458, amb3672, amb3734, amb3742, amb3766, amb4107, amb4111, amb4543	[*Matsunaga et al.*, 2005; *Wahyudi et al.*, 2001]
MSR-1	Mini-Tn5	?	2	AAX11190 (CheY) (~amb0983)	[*Li et al.*, 2005]
AMB-1	Mariner	700	2	amb0968 (mamN), amb0972 (mamQ)	[*Komeili et al.*, 2004]
AMB-1	Mariner	5809	19	amb0089, amb0172, amb0200, amb0516, amb3233, amb0963 (mamE), amb0967 (mamM), amb0968 (mamN), amb0969 (mamO), amb0971 (mamA), amb0972 (mamQ)	This Study

Chapter 3: Environmental Microbiology

3.1. Extremophilic Magnetotactic Bacteria and Archaea

Nash, C. Z.[1], Popa, R.[2], Kobayashi, A.[3], and J. L. Kirschvink[1]

[1]*Division of Geological and Planetary Sciences, California Institute of Technology, Pasadena, CA, 91125, USA.* [2]*Portland State University, Portland, OR, 97207, USA.* [3]*Photonics Research Institute, National Institute of Advanced Industrial Science and Technology, Osaka, Japan.*

Magnetotactic bacteria (MB) form nanoscale crystals of the ferrimagnetic minerals magnetite (Fe_3O_4) or greigite (Fe_3S_4) inside intracellular lipid-membrane-bounded vesicles termed magnetosomes. All reports since their initial discovery [*Blakemore,* 1975] have been in freshwater, marine, and soil environments at near neutral pH and temperatures below 30° C [*Bazylinski and Frankel,* 2004]. Only two of the 150+ 16S rDNA sequences of MB lie outside of the bacterial phylum Proteobacteria. These two belong to the genus Magnetobacterium in the phylum Nitrospirae. In order to better understand the diversity and environmental range of MB we examined samples from two extreme environments. Here we report the discovery of several magnetotactic extremophiles: a thermophile from Little Hot Creek (LHC), (37.69º N, 118.84º W), and four from the hyper-alkaline, hyper-saline waters of Mono Lake (37.98º N 119.12º W). Analysis of the 16S rRNA gene indicates that the thermophilic organism groups with the genus Magnetobacterium in the phylum Nitrospirae, whereas one species of MB from Mono Lake (MonoEub) lies with the γ-proteobacteria. We also report the first evidence for magnetotactic Archaea, in three clones from Mono Lake: ML1, ML3, and ML4. Our findings

extend the environmental range of these fossil-forming organisms to include environments expected to have existed on early Earth and will facilitate geo- and astrobiological investigations. Our findings also extend the phylogenetic breadth of magnetotactic microorganisms to include all three domains of life. We anticipate these organisms to be targets for further analysis to investigate the evolution and origins of magnetotaxis.

We conducted an initial survey of the LHC site by taking 10 microliter samples with a pipette and checking them microscopically for a response to a magnetic field. We checked a range of temperatures from 40º to 80º C at every spring within the group. We only observed magnetotactic bacteria at one freshwater spring, in 45º–55º C mats adjacent to the main flow channel. These microbial mats were ~ 1 cm thick, dominated by a red layer on the surface. We observed MB throughout these mats, but in higher densities ~ 5 mm from the surface. Microscopic examination of biofilms from similar hot springs in central California revealed the presence of MB in microbial mats at temperatures up to 58º C.

We collected small cores of mats and sediments that were kept at 50º C during transport to, and in, the lab. We observed MB bacteria in these samples over several months, indicating that they are able to live at these temperatures. Using the magnetic racetrack technique [*Wolfe et al.*, 1987], we then isolated pellets of MB. We amplified, cloned, and sequenced DNA using standard techniques, employing either universal bacterial or archaeal primers. RFLP analysis of 6–10 clones from each sample showed they were homogenous. Phylogenetic analysis of the sequences obtained was carried out

with ARB (see Figure 1). The LHC sequences belong to a group of Nitrospirae that contains two other MB, as well as clones from other hot springs (see Figure 2).

Samples from Mono Lake (pH of 9.8 and salinity 80.8 g/l) were collected from the shore to depths up to 40 m using a gravity corer or SCUBA. Cores were stored at room temperature and MB were observed over a period of months. MB were extracted and analyzed as with the LHC samples. The closest relatives of the archaeal sequences are clones from deep-sea hydrothermal surveys, while the closest relatives to the MonoEub sequence are from Mono Lake and other basic, salty locales (see Figures 3–5).

HRTEM and HAADF/STEM/EDX examination (Tecnai F20 G2Twin) of these organisms revealed prismatic or bullet-shaped magnetite crystals organized in string-like bundles; no Greigite magnetosomes were detected (see Figures 6 and 7). The ability of these bacteria to form magnetite in extremes of temperature, salinity and alkalinity may prove useful in manufacturing magnetic nanoparticles for many existing applications [*Šafarík and Šafaríková*, 2002].

As the deepest branches of the tree of life are composed of thermophiles, these discoveries, coupled with the wide phyletic distribution of magnetite-precipitating organisms shown in Figure 1, indicate that magnetotaxis could be a very ancient trait, perhaps even pre-dating the divergence of the Bacterial, Archaeal, and Eukaryal Domains.

Sediments of hydrothermal origin are known in the geological record as far back as 3.5 Ga [*Brasier et al.*, 2002], so there is the potential for tracing the fossil remains of these bacteria into Archean time. Currently unequivocal magnetofossils have been found in sediments dating back to the Cretaceous, and potential ones as old as the

Paleoproterozoic [*Chang et al.*, 1989; *Kopp and Kirschvink*, 2008]. The ability to identify these biomarkers in environments found on the early Earth and thought to exist elsewhere in the universe provides a new tool to look for ancient and alien life.

Author Contributions C.Z.N., R.P., and J.L.K. performed the sampling. C.Z.N. performed the molecular and phylogenetic work. A.K.K. performed the electron microscopy. All authors discussed the results and commented on the manuscript.

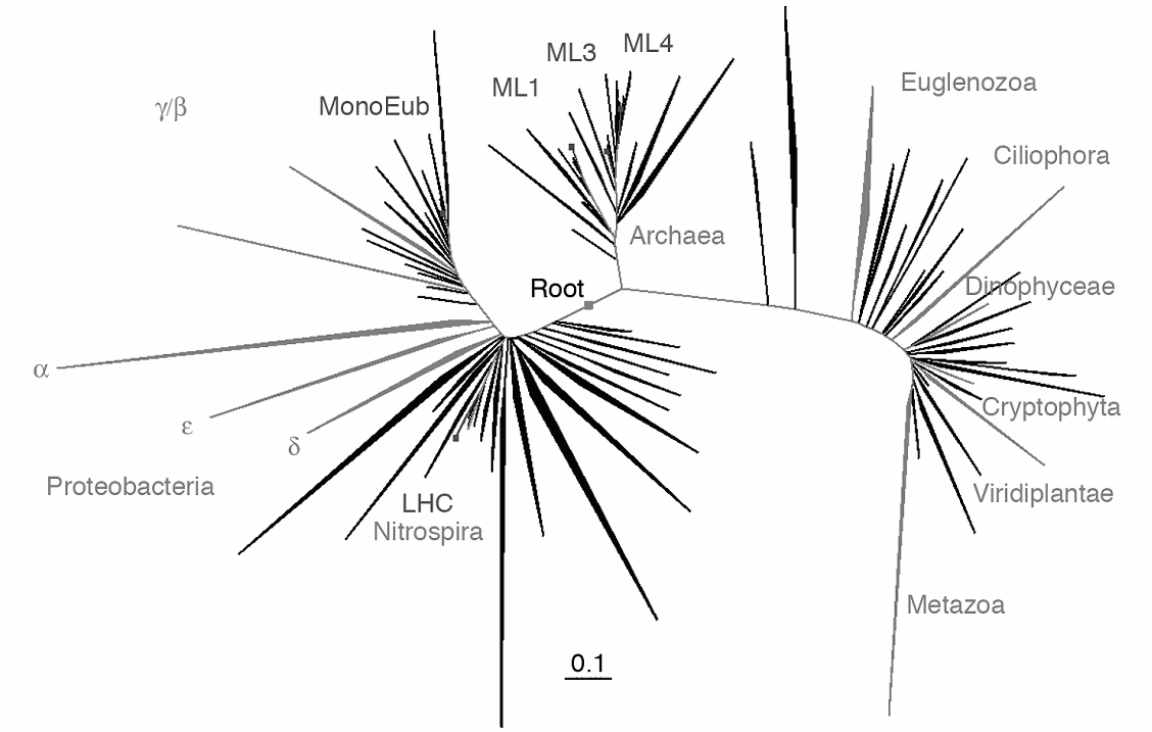

Figure 1: Small subunit rRNA phylogenetic tree. Groups containing species which synthesize magnetic minerals highlighted in grey and labelled. Sequences obtained from this study shown in dark grey.

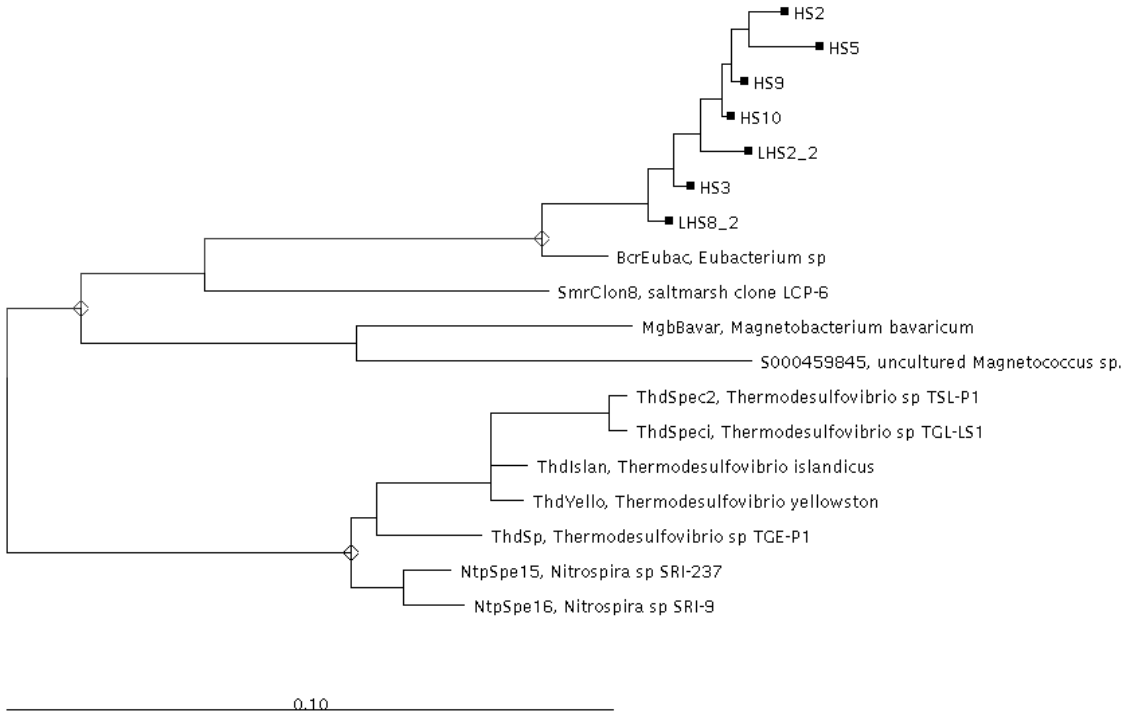

Figure 2: Phylogenetic tree of 16S rRNA sequences closest to the magnetotactic bacterial sequence obtained from Little Hot Creek, CA. They fall into the Nitrospirae phylum, a diverse group of nitrite oxidizing, sulfate reducing organisms from contaminated and thermal environments. The closest clone to our sequences, BcrEubac, is from the outflow channel of Octopus Springs, Yellowstone National Park, WY [*Kopczynski et al.*, 1994]. Saltmarsh clone LCP-6 is an unpublished sequence from a contaminated site. The next two closest relatives are both MB from lakes in Bavaria [*Flies et al.*, 2005; *Spring et al.*, 1993]. Note the closest isolates are *Thermodesulfovibrio spp.* from hot springs in Yellowstone and Iceland. Tree was constructed using ARB, with alignments manually curated and sequences added to the tree in interactive parsimony mode [*Ludwig et al.*, 2004].

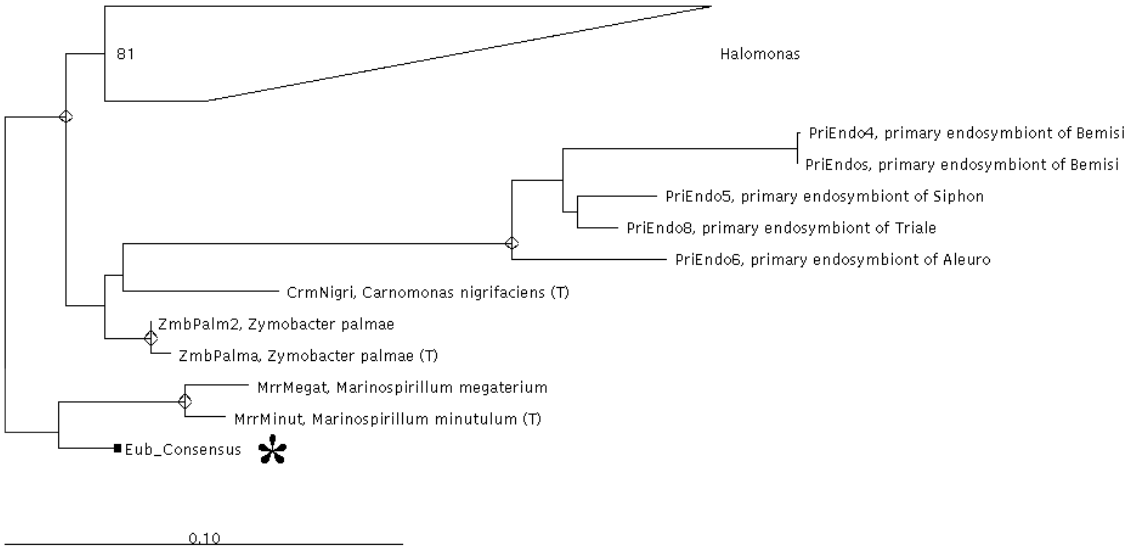

Figure 3: Phylogenetic tree of 16S rRNA sequences closest to the magnetotactic bacterial sequence obtained from Mono Lake, CA, marked with the asterisk. Note the closest isolates are *Marinospirillum minutulum* and *M. megaterium*, both from a low oxygen, high nitrogen, moderate salinity environment — a fermented brine [*Satomi et al.*, 1998]. Tree was constructed using ARB, with alignments manually curated and sequences added to the tree in interactive parsimony mode [*Ludwig et al.*, 2004].

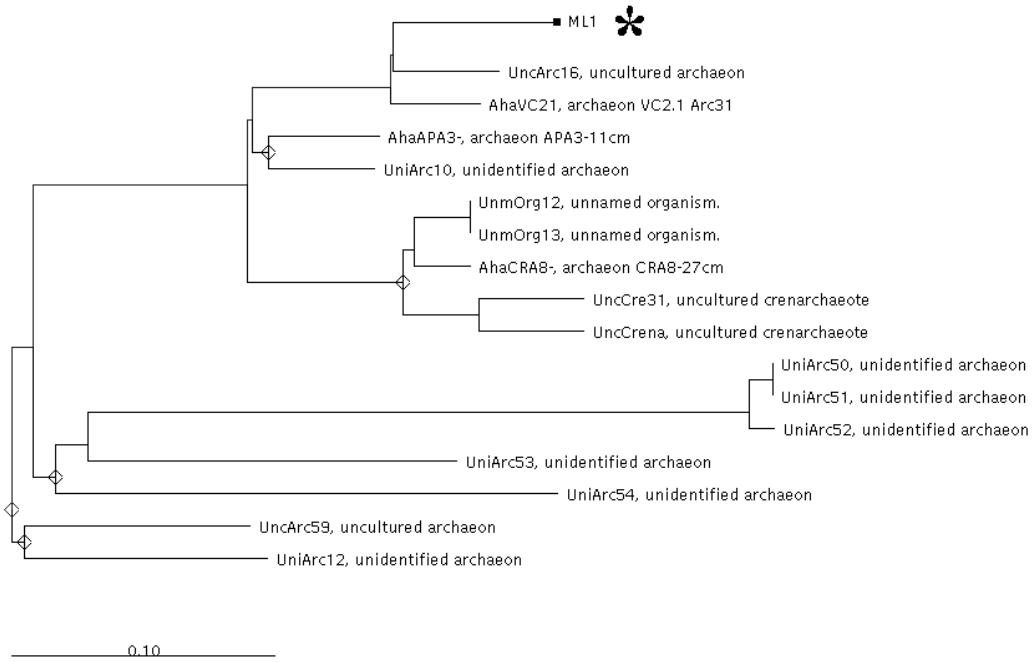

Figure 4: Phylogenetic tree of 16S rRNA sequences closest to the first putative archaeal sequence obtained from Mono Lake, CA, marked with the asterisk. There are no isolates closely related to ML1. The nearby clones, UncArc16 and AhaVC21, are both from deep sea hydrothermal vent samples and belong to marine benthic group B [*Reysenbach et al.*, 2000; *Teske et al.*, 2002]. This tree was constructed using ARB, with alignments manually curated and sequences added to the tree in interactive parsimony mode [*Ludwig et al.*, 2004].

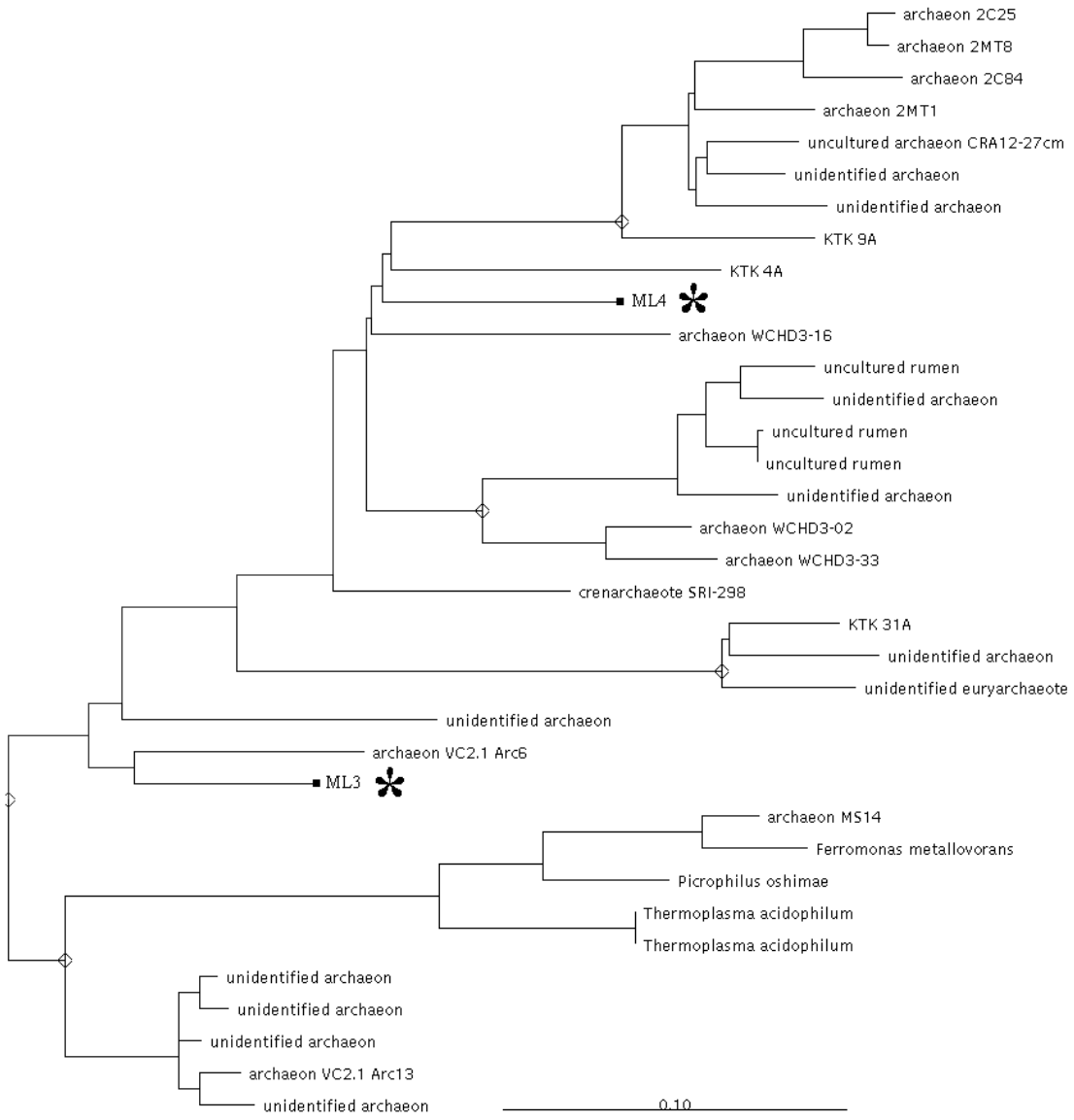

Figure 5: Phylogenetic tree of 16S rRNA sequences closest to the other putative archaeal sequences obtained from Mono Lake, CA, marked with the asterisk. There are no isolates closely related to either ML3 or ML4. ML3's neighbors, VC2.1 Arc6 and an unidentified archaeon are both from deep sea hydrothermal vent samples [*Reysenbach et al.*, 2000; *Takai and Horikoshi*, 1999]. ML4's neighbors are single clone from the methanogenic zone of a contaminated sediment (WCHD3-16, [*Dojka et al.*, 1998]) and a

dominant clone from high salinity, deep sea brines (KTK4A, [*Eder et al.*, 1999]). The nearest isolates are *Thermoplasma acidophilum* and *Picrophilus oshimae*, both meso- to thermophilic acidophiles [*Golyshina and Timmis*, 2005]. This tree was constructed using ARB, with alignments manually curated and sequences added to the tree in interactive parsimony mode [*Ludwig et al.*, 2004].

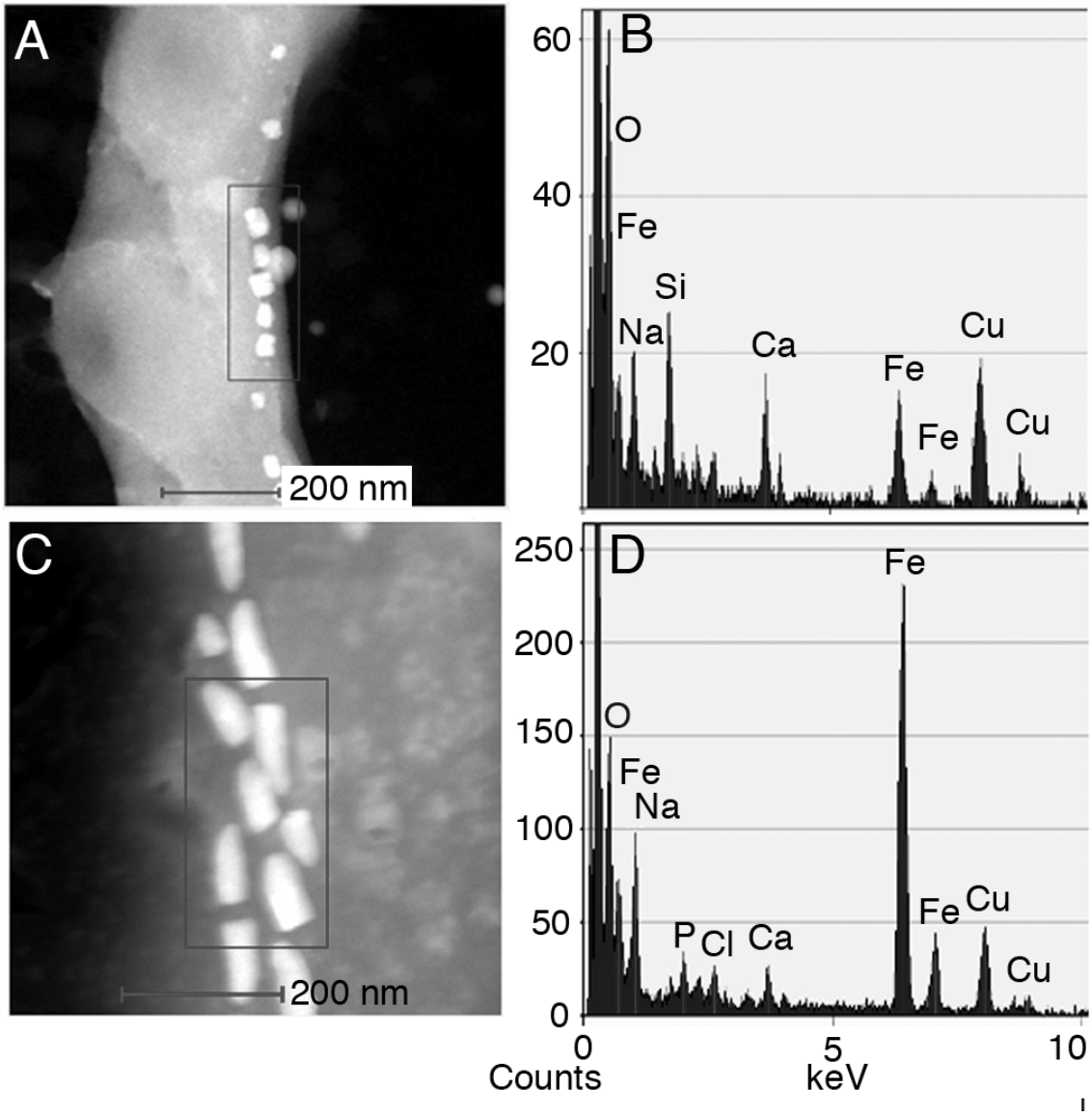

Figure 6: HAADF/EDX of ML and LHC samples. (A) HAADF image of Mono Lake sample. Region boxed in red analyzed with EDX. (B) EDX Analysis of sample from Mono Lake shows Fe and O, suggesting magnetite. (C) HAADF image of LHC sample. (D) EDX analysis of sample from LHC shows Fe and O, suggesting magnetite.

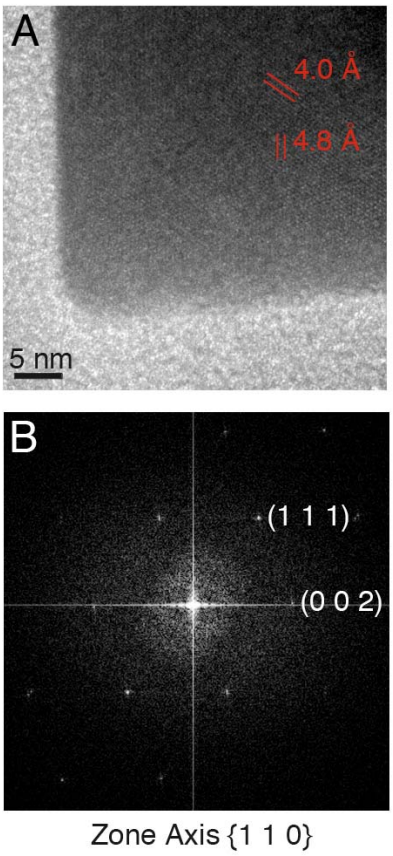

Figure 7: HRTEM/FFT of LHC sample. (A) HRTEM from one of LHC crystals in 2C showing lattice spacing characteristic of magnetite (B) Fast Fourier Transform pattern of the crystal in A confirms magnetite.

Chapter 3: Environmental Microbiology

3.2. Degenerate PCR recovery of *mamB* fragment from LA Arboretum magnetic cocci.

3.2.1. Introduction

The phylogenetic distribution of MB includes all of the phyla Nitrospirae, Proteobacteria, and possibly even Firmicutes. Genes which are known to be involved in magnetosome formation have so far only been retrieved from three magnetospirilla and one magnetic coccus (strain MC-1), all of which are in the α-Proteobacteria. This project was an effort to retrieve some of these genes from other MB.

For this we chose two targets. The first was a magnetic cocci found in the Los Angeles Arboretum tentatively named ARB-1 [*Cox et al.*, 2002]. ARB-1 was chosen both because of its great abundance in the environment and because of its phylogenetic position. ARB-1 is distant from both MC-1 and the magnetospirilla, yet still within the magnetic coccus clade of the α-Proteobacteria.

The second target is *Desulfovibrio magneticus* RS-1 [*Sakaguchi et al.*, 1993; *Sakaguchi et al.*, 2002]. RS-1 is a δ-Proteobacteria and the only MB in pure culture which is not an α-Proteobacteria.

The genes chosen were *mamA, mamB,* and *mamC*. These genes were chosen because of their presence in both the magnetospirilla and MC-1 and their position at the beginning of the *mam* cluster, which encodes many of the proteins that are abundant in the magnetosome membrane. More recent work on *mamA* and *mamC* has demonstrated

that these genes affect the number and shape of crystals in the magnetospirilla, but are not necessary for magnetite formation [*Komeili et al.*, 2004; *Scheffel et al.*, 2008].

3.2.2. Methods

Enrichment of ARB-1

Sediment samples were collected from Lake Baldwin in the Los Angeles Arboretum in Arcadia, CA. Magnetic cocci were observed to be in the highest abundance in the most sapropelic muds, based on hanging drop observations. MB were enriched by placing magnets on the outside of the sample bottles, shaking the jar until all sediment was suspended and then allowing it to settle for 2 hours. 1 ml of water and magnetic material was collected from each the north and south magnets and run over superparamagnetic columns (Miltenyi Biotec, Germany). 10 ml aliquots of 0.2 μm filtered sample water were used to rinse non-MB from the column; washing was carried out five times until no bacteria were observed in the elution. The magnets were then removed from the column and two 10 ml aliquots of 0.2 μm filtered sample water were flushed through to collect the MB. Samples were centrifuged and re-suspended in 1 ml of the original supernatant. DNA was then extracted from the sample using an Ultraclean Soil DNA Kit (Mo Bio Laboratories, USA).

RS-1

Desulfovibrio magneticus RS-1 was obtained from the DSMZ (Germany) and cultured anaerobically as described previously [*Sakaguchi et al.*, 2002]. DNA was extracted using a standard phenol-chloroform extraction [*Sambrook et al.*, 1989].

Degenerate PCR

Degenerate primers were designed based on the *mamA, mamB,* and *mamC* sequences from MS-1 and MC-1 using the CODEHOP software [*Rose et al.,* 1998]. Various PCR conditions were tested. Promega 2X reaction solution was used with 1–10 μL of template DNA, with 30–50 amplification cycles, with annealing temperatures of 52–58˚ C. Products were purified with QIAGEN gel extraction kit, cloned with TOPO TA 2.1 cloning vector into DH5α cells, and minipreped with QIAGEN miniprep kit for sequencing.

Primers Used:

Adeg4 5' TGAATGATGATTATCGTCAGGTGTATTATmgngayaargg 3'

Adeg5 5' GATTATCGTCAGGTGTATTATCGTgayaarggnat 3'

Adeg6R 5' CCATGCCCAGACGATAATGAayrttraartt 3'

Adeg7R 5' CTGAAAGGCATCAATCgcytcrtcrwa 3'

Bdeg1 5' CCCTGAAAATTTCCAACAGAccngcngayga 3'

Bdeg2 5' CGGCGATTATGGCGaaygcntggga 3'

Bdeg3 5' GCGATTATGGCGAACgcntgggayaa 3'

Bdeg4 5' GGCGAACGCGtgggayaaymg 3'

Bdeg5R 5' CATCGGAACGGTTAtcccangcrtt 3'

Bdeg6R 5' AACGCATCGGAACGGttrtcccangc 3'

Bdeg7R 5' GAGGAAAACGCATCGGAAckrttrtccca 3'

Bdeg8R 5' CCAAAGGTGGCAAAAATCacnccnaycat 3'

Bdeg9R 5' CCGGGGAGGCAtccatnarncc 3'

Cdeg1 5' ACCAACACAGAAGCGGTGathgayacngg 3'

Cdeg2 5' CAACACAGAAGCGGTGATTgayacnggnaa 3'

Cdeg3 5' AACACAGAAGCGGTGATTGATacnggnaarga 3'

Cdeg4 5' AAGCGGTGATTGATACCggnaargarrc 3'

Cdeg5R 5' TGATCCATGCCATAATCCcangcrtaytt 3'

Cdeg6R 5' TGATCCATGCCATAATcccangcrtayt 3'

Cdeg7R 5' TGATCCATGCCATAAtcccangcrta 3'

3.2.3. Results and Discussion

After magnets were left on the shaken sample jar for two hours, 1 ml samples were taken. Approximately 10^3 magnetic cocci were observed in the 10 μL sub-samples, or ~ 10^5 total magnetic cocci (see Figure 8a). After running onto the magnetic column and flushing five times, no bacteria were visible in the elutant (see Figure 8b–c). The magnets were removed from the column and washed twice, yielding ~ 10^4 magnetic cocci per ml (see Figure 8d). The sample was centrifuged and resuspended in $1/20^{th}$ of the supernatant (see Figure 8e) and then checked for non-magnetotactic cells (see Figure 9).

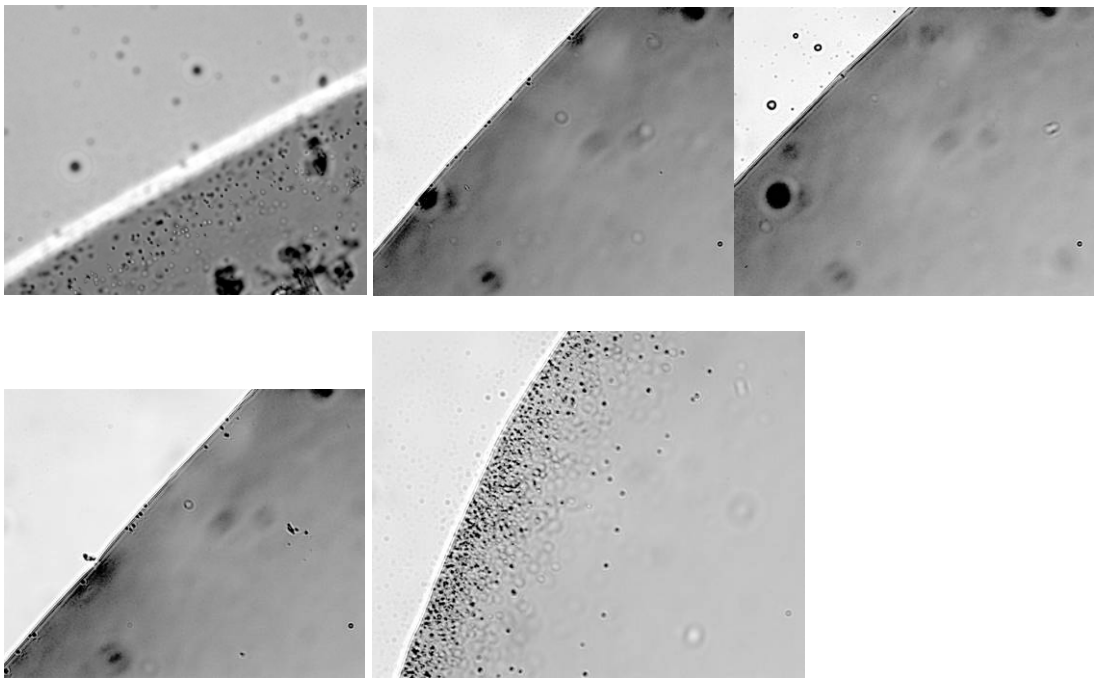

Figure 8: Enrichment of magnetic cocci: (a) un-enriched sample; (b) 1st negative selection; (c) 5th negative selection; (d) positive selection; (e) 20x concentrated positive selection

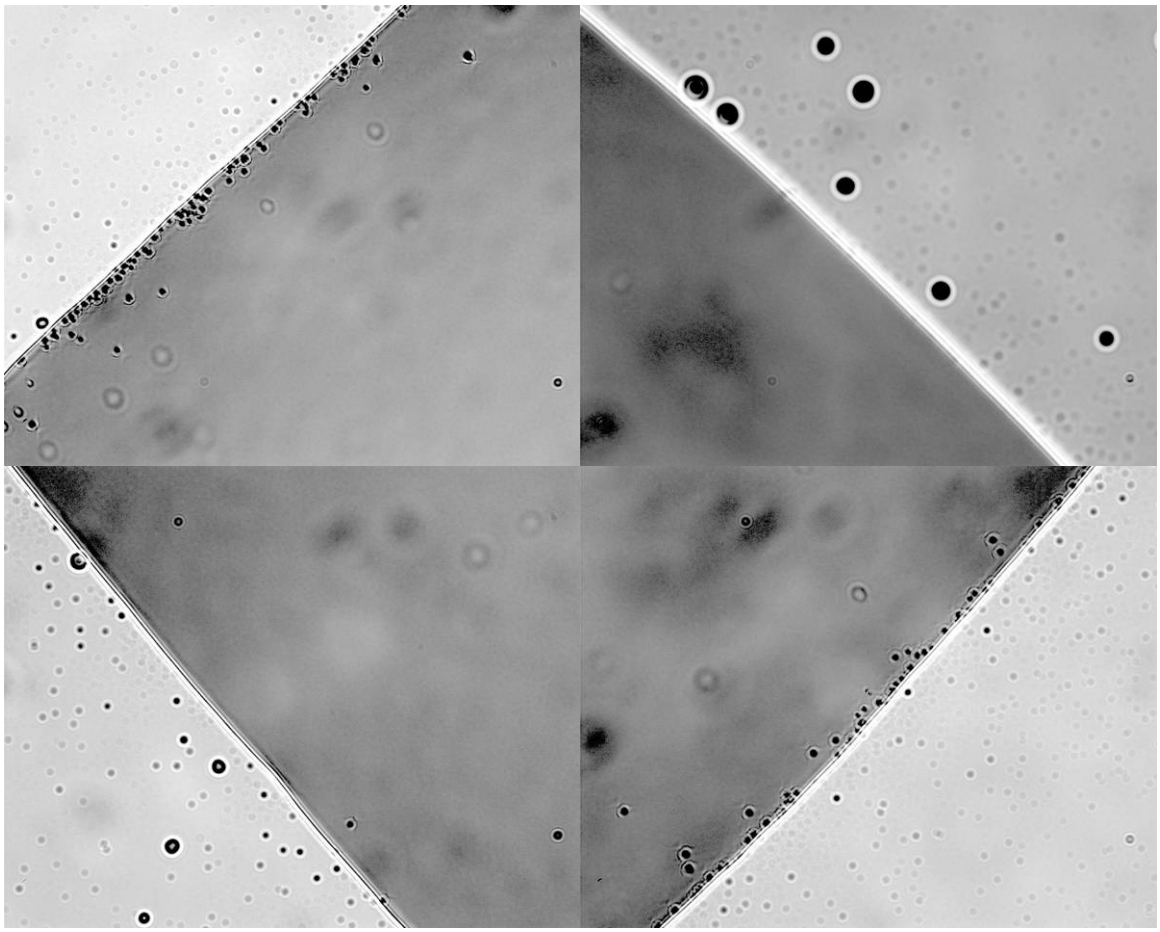

Figure 9: Checking sample for non-magnetotactic bacteria. The applied field is towards the top left of the image. Note the population of south-seeking MB, as previously observed [*Cox et al.*, 2002].

Degenerate PCR

Numerous products were obtained, but by screening the PCR products for the expected size most false positives could be excluded. The rest were examined by sequencing. Some of the false positives obtained on sequencing had no similarity to any genes from MB at either the DNA or protein level and included fragments which best matched a xanthine/uracil permease from *Pseudomonas fluorescens*, a hypothetical

protein from *Nostoc punctiformis,* and a glycosyltransferase from *Geobacter metallireducens.* The degenerate primers for *mamA* repeatedly recovered fragments that were > 95% identical to sequences from the magnetospirilla. This is likely due to magnetospirilla being present in the magnetically enriched samples from which DNA was extracted. It is also possible the arboretum magnetic cocci have Magnetospirillum versions of their *mamA* gene. This could be determined through larger scale sequencing or probing for the *mamA* gene and the 16S rRNA gene with fluorescent probes. The degenerate primers for *mamC* failed to amplify any products of the expected size.

The primer Bdeg1 with either Bdeg5R or Bdeg7R was able to retrieve a 247 bp sequence whose translation is 80% similar to the MC-1 MamB and 73% similar to the MS-1 MamB protein. MamB is a protein known to localize to the magnetosome [*Grünberg et al.*, 2001] and is predicted to be a heavy metal transporter similar to the cobalt/zinc/cadmium transporter CzcD. The arboretum MamB sequence groups with the MamB genes from magnetotactic bacteria, and broadly follows the 16S rDNA gene phylogeny (see Figure 10). Note that although it broadly follows the 16S tree, there are clear instances of LGT: *Porphyromonas* has an archaeal version, *Methanococcus* and *Pyrococcus* have a bacterial version. Also note MS-1 has one close duplicate and MC-1 has two duplicates.

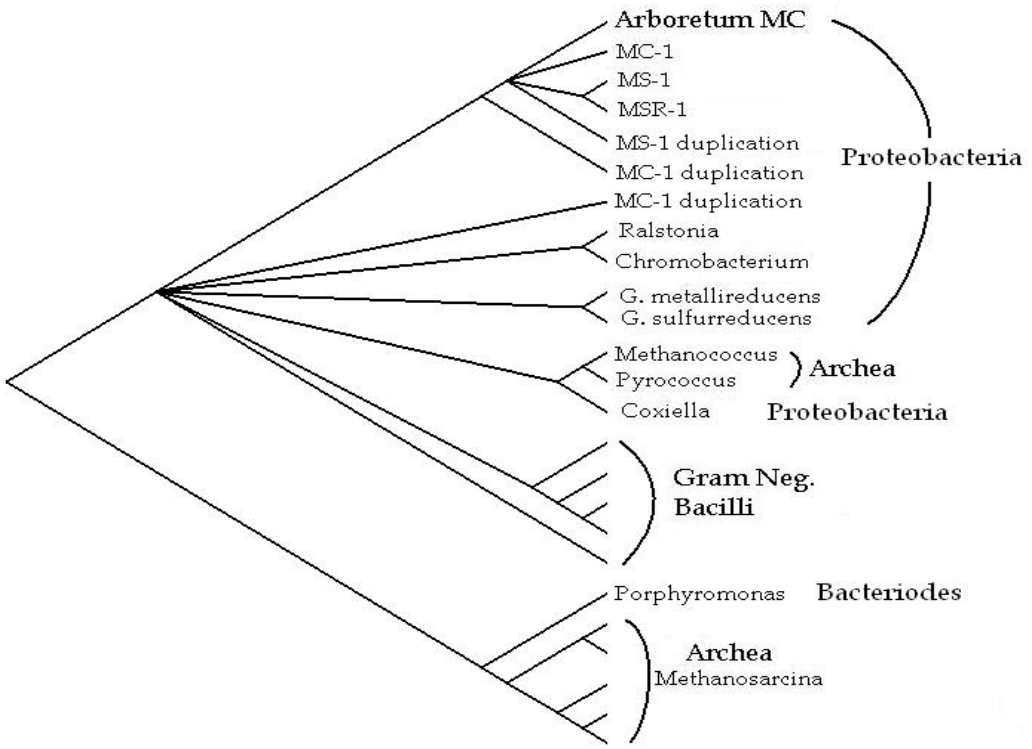

Figure 10: Phylogeny of MamB and CzcD proteins. This is a strict-consensus tree of 100 bootstrap replicates of a Neighbor-Joining/Distance tree using the Kimura 2-parameter correction with 301 characters in the alignment, made using the PHYLIP package. Branches with less than 90% bootstrap support were collapsed. The scale is arbitrary, only branching order is informative.

References

Abe, M., et al. (1999), Magnetite Film Growth at 30°C on Organic Monomolecular Layer, Mimicking Bacterial Magnetosome Synthesis, *Journal of Applied Physics*, *85*(8), 5705–5707.

Altschul, S. F., et al. (1997), Gapped BLAST and PSI-BLAST: A New Generation of Protein Database Search Programs, *Nucleic Acids Research*, *25*(17), 3389–3402.

Arakaki, A., et al. (2003), A Novel Protein Tightly Bound to Bacterial Magnetic Particles in *Magnetospirillum magneticum* strain AMB-1, *Journal of Biological Chemistry*, *278*(10), 8745–50.

Balkwill, D. L., et al. (1980), Ultrastructure of a Magnetotactic Spirillum, *Journal of Bacteriology*, *141*(3), 1399–1408.

Bazylinski, D. A., and R. B. Frankel (2004), Magnetosome Formation in Prokaryotes, *Nature Reviews Microbiology*, *2*, 217–230.

Bertani, L. E., et al. (2001), Physical and genetic characterization of the genome of *Magnetospirillum magnetotacticum*, strain MS-1, *Gene*, *264*(2), 257–263.

Blakemore, R. (1975), Magnetotactic Bacteria, *Science*, *190*(4212), 377–379.

Blakemore, R. P., et al. (1979), Isolation and Pure Culture of a Freshwater Magnetic Spirillum in Chemically Defined Medium, *Journal of Bacteriology*, *140*(2), 720–729.

Boskey, A. L. (1998), Biomineralization: Conflicts, challenges, and opportunities, *Journal of Cellular Biochemistry*, *30–31*, 83–91.

Brasier, M. D., et al. (2002), Questioning the evidence for Earth's oldest fossils, *Nature*, *416*(6876), 76–81.

Chang, S. B. R., et al. (1989), Biogenic Magnetite in Stromatolites .2. Occurrence in Ancient Sedimentary Environments, *Precambrian Research*, *43*(4), 305–315.

Chiang, S. L., and E. J. Rubin (2002), Construction of a mariner-based transposon for epitope-tagging and genomic targeting, *Gene*, *296*(1–2), 179–85.

Cox, B. L., et al. (2002), Organization and elemental analysis of P-, S-, and Fe-rich inclusions in a population of freshwater magnetococci, *Geomicrobiology Journal*, *19*(4), 387–406.

Dean, A. J., and D. A. Bazylinski (1999), Genome analysis of several marine, magnetotactic bacterial strains by pulsed-field gel electrophoresis, *Current Microbiology*, *39*(4), 219–225.

Dehio, C., and M. Meyer (1997), Maintenance of broad-host-range incompatibility group P and group Q plasmids and transposition of Tn5 in *Bartonella henselae* following conjugal plasmid transfer from *Escherichia coli*., *Journal of Bacteriology*, *179*(2), 538–40.

Delong, E. F., et al. (1993), Multiple Evolutionary Origins of Magnetotaxis in Bacteria, *Science*, *259*(5096), 803–806.

Dojka, M. A., et al. (1998), Microbial diversity in a hydrocarbon- and chlorinated-solvent-contaminated aquifer undergoing intrinsic bioremediation, *Applied and Environmental Microbiology*, *64*(10), 3869–3877.

Eder, W., et al. (1999), Novel 16S rRNA gene sequences retrieved from highly saline brine sediments of Kebrit Deep, Red Sea, *Archives of Microbiology*, *172*(4), 213–218.

Flies, C. B., et al. (2005), Diversity and vertical distribution of magnetotactic bacteria along chemical gradients in freshwater microcosms, *FEMS Microbiology Ecology*, *52*(2), 185–195.

Fontecave, M., et al. (2004), S-adenosylmethionine: nothing goes to waste, *Trends in Biochemical Sciences*, *29*(5), 243–249.

Frankel, R. B., et al. (1983), Fe_3O_4 Precipitation in Magnetotactic Bacteria, *Biochimica Et Biophysica Acta*, *763*(2), 147–159.

Frankel, R. B., and D. A. Bazylinski (1994), Magnetotaxis and Magnetic Particles in Bacteria, *Hyperfine Interactions*, *90*(1–4), 135–142.

Frankel, R. B., et al. (1997), Magneto-aerotaxis in marine coccoid bacteria, *Biophysical Journal*, *73*(2), 994–1000.

Glasauer, S., et al. (2002), Intracellular iron minerals in a dissimilatory iron-reducing bacterium, *Science*, *295*(5552), 117–119.

Golyshina, O. V., and K. N. Timmis (2005), Ferroplasma and relatives, recently discovered cell wall-lacking archaea making a living in extremely acid, heavy metal-rich environments, *Environmental Microbiology*, *7*(9), 1277–1288.

Grünberg, K., et al. (2001), A Large Gene Cluster Encoding Several Magnetosome Proteins is Conserved in Different Species of Magnetotactic Bacteria, *Applied and Environmental Microbiology*, *67*(10), 4573–4582.

Grünberg, K., et al. (2004), Biochemical and proteomic analysis of the magnetosome membrane in *Magnetospirillum gryphiswaldense*, *Applied and Environmental Microbiology*, *70*(2), 1040–1050.

Guerin, W. F., and R. P. Blakemore (1992), Redox Cycling of Iron Supports Growth and Magnetite Synthesis by Aquaspirillum magnetotacticum, *Applied and Environmental Microbiology*, *58*(4), 1102–1109.

Handrick, R., et al. (2004), Unraveling the function of the Rhodospirillum rubrum activator of polyhydroxybutyrate (PHB) degradation: the activator is a PHB-granule-bound protein (phasin), *Journal of Bacteriology*, *186*(8), 2466–2475.

Kawaguchi, R., et al. (1995), Phylogenetic Analysis of a Novel Sulfate-Reducing Magnetic Bacterium, RS-1, Demonstrates its Membership of the δ-Proteobacteria, *FEMS Microbiology Letters*, *126*(3), 277–282.

Kirschvink, J. L., and H. A. Lowenstam (1979), Mineralization and Magnetization of Chiton Teeth — Paleomagnetic, Sedimentologic, and Biologic Implications of Organic Magnetite, *Earth and Planetary Science Letters*, *44*(2), 193–204.

Kirschvink, J. L. (1980), South-Seeking Magnetic Bacteria, *Journal of Experimental Biology*, *86*(JUN), 345–347.

Kirschvink, J. L. (1982), Paleomagnetic Evidence for Fossil Biogenic Magnetite in Western Crete, *Earth and Planetary Science Letters*, *59*(2), 388–392.

Kobayashi, A., et al. (2006), Experimental observation of magnetosome chain collapse in magnetotactic bacteria: Sedimentological, paleomagnetic, and evolutionary implications, *Earth and Planetary Science Letters*, *245*(3–4), 538–550.

Komeili, A., et al. (2004), Magnetosome vesicles are present before magnetite formation, and MamA is required for their activation, *Proceedings of the National Academy of Sciences of the United States of America*, *101*(11), 3839–3844.
Komeili, A., et al. (2006), Magnetosomes are cell membrane invaginations organized by the actin-like protein MamK, *Science*, *311*(5758), 242–245.
Kopczynski, E. D., et al. (1994), Recognition of chimeric small subunit ribosomal DNAs composed of genes from uncultivated microorganisms, *Applied and Environmental Microbiology*, *60*(2), 746–748.
Kopp, R. E., and J. L. Kirschvink (2008), The identification and biogeochemical interpretation of fossil magnetotactic bacteria, *Earth-Science Reviews*, *86*(1–4), 42–61.
Layer, G., et al. (2004), Structure and function of radical SAM enzymes, *Current Opinion in Chemical Biology*, *8*(5), 468–476.
Levi-Kalisman, Y., et al. (2001), Structure of the nacreous organic matrix of a bivalve mollusk shell examined in the hydrated state using Cryo-TEM, *Journal of Structural Biology*, *135*(1), 8–17.
Li, F., et al. (2005), Cloning and functional analysis of the sequences flanking mini-Tn5 in the magnetosomes deleted mutant NM6 of Magnetospirillum gryphiswaldense MSR-1, *Science in China Series C-Life Sciences*, *48*(6), 574–584.
Ludwig, W., et al. (2004), ARB: a software environment for sequence data, *Nucleic Acids Research*, *32*(4), 1363–1371.
Maness, P. C., and P. F. Weaver (2001), Evidence for three distinct hydrogenase activities in *Rhodospirillum rubrum*, *Applied Microbiology and Biotechnology*, *57*(5–6), 751–6.
Mann, S., et al. (1984), Structure, Morphology and Crystal-Growth of Bacterial Magnetite, *Nature*, *310*(5976), 405–407.
Mann, S., et al. (1990), Magnetotactic Bacteria — Microbiology, Biomineralization, Paleomagnetism and Biotechnology, *Advances in Microbial Physiology*, *31*, 125–181.
Matsunaga, T., et al. (1991), Magnetite Formation by a Magnetic Bacterium Capable of Growing Aerobically, *Applied Microbiology and Biotechnology*, *35*(5), 651–655.
Matsunaga, T., et al. (1992), Gene-Transfer in Magnetic Bacteria — Transposon Mutagenesis and Cloning of Genomic DNA Fragments Required for Magnetosome Synthesis, *Journal of Bacteriology*, *174*(9), 2748–2753.
Matsunaga, T., et al. (2005), Complete genome sequence of the facultative anaerobic magnetotactic bacterium Magnetospirillum sp strain AMB-1, *DNA Research*, *12*(3), 157–166.
Meldrum, F. C., et al. (1993), Electron-Microscopy Study of Magnetosomes in a Cultured Coccoid Magnetotactic Bacterium, *Proceedings of the Royal Society of London Series B—Biological Sciences*, *251*(1332), 231–236.
Metcalf, W. W., et al. (1996), Conditionally Replicative and Conjugative Plasmids Carrying *lacZa* for Cloning, Mutagenesis, and Allele Replacement in Bacteria, *Plasmid*, *35*, 1–13.

Nakamura, C., et al. (1995), An Iron-Regulated Gene, *magA*, Encoding an Iron Transport Protein of *Magnetospirillum* sp. Strain AMB-1, *Journal of Biological Chemistry*, *270*(47), 28392–28396.

Noguchi, Y., et al. (1999), Iron reductase for magnetite synthesis in the magnetotactic bacterium Magnetospirillum magnetotacticum, *Journal of Bacteriology*, *181*(7), 2142–2147.

Ofer, S., et al. (1984), Magnetosome Dynamics in Magnetotactic Bacteria, *Biophysical Journal*, *46*(1), 57–64.

Paoletti, L. C., and R. P. Blakemore (1988), Iron Reduction by Aquaspirillum magnetotacticum, *Current Microbiology*, *17*(6), 339–342.

Pereira-Mouries, L., et al. (2002), Soluble silk-like organic matrix in the nacreous layer of the bivalve Pinctada maxima, *European Journal of Biochemistry*, *269*(20), 4994–5003.

Raymond, J., et al. (2002), Whole-Genome Analysis of Photosynthetic Prokaryotes, *Science*, *298*, 1616–1620.

Reysenbach, A. L., et al. (2000), Novel bacterial and archaeal lineages from an in situ growth chamber deployed at a Mid-Atlantic Ridge hydrothermal vent, *Applied and Environmental Microbiology*, *66*(9), 3798–3806.

Richter, M., et al. (2007), Comparative genome analysis of four magnetotactic bacteria reveals a complex set of group-specific genes implicated in magnetosome biomineralization and function, *Journal of Bacteriology*, *189*(13), 4899–4910.

Rose, T. M., et al. (1998), Consensus-degenerate hybrid oligonucleotide primers for amplification of distantly related sequences, *Nucleic Acids Research*, *26*(7), 1628–1635.

Šafarík , I., and M. Šafaríková (2002), Magnetic Nanoparticles and Biosciences, *Monatshefte Fur Chemie*, *133*(6), 737–759.

Sakaguchi, T., et al. (1993), Magnetite Formation by a Sulfate-Reducing Bacterium, *Nature*, *365*(6441), 47–49.

Sakaguchi, T., et al. (2002), *Desulfovibrio magneticus* sp. nov., a novel sulfate-reducing bacterium that produces intracellular single-domain-sized magnetite particles, *International Journal of Systematic and Evolutionary Microbiology*, *52*, 215–221.

Sakane, T., and A. Yokota (1994), Chemotaxonomic Investigation of Heterotrophic, Aerobic and Microaerophilic Spirilla, the Genera Aquaspirillum, Magnetospirillum and Oceanospirillum, *Systematic and Applied Microbiology*, *17*(1), 128–134.

Sambrook, J., et al. (1989), *Molecular cloning: a laboratory manual*, 2nd ed., Cold Spring Harbor Laboratory Press, Cold Spring Harbor, NY.

Satomi, M., et al. (1998), Marinospirillum gen. nov., with descriptions of Marinospirillum megaterium sp. nov., isolated from kusaya gravy, and transfer of Oceanospirillum minutulum to Marinospirillum minutulum comb. nov, *International Journal of Systematic Bacteriology*, *48*, 1341–1348.

Scheffel, A., et al. (2006), An acidic protein aligns magnetosomes along a filamentous structure in magnetotactic bacteria, *Nature*, *440*(7080), 110–114.

Scheffel, A., et al. (2008), The major magnetosome proteins MamGFDC are not essential for magnetite biomineralization in Magnetospirillum gryphiswaldense but

regulate the size of magnetosome crystals, *Journal of Bacteriology*, *190*(1), 377–386.

Schübbe, S., et al. (2003), Characterization of a Spontaneous Nonmagnetic Mutant of *Magnetospirillum gryphiswaldense* Reveals a Large Deletion Comprising a Putative Magnetosome Island, *Journal of Bacteriology*, 5779–5790.

Spring, S., et al. (1993), Dominating Role of an Unusual Magnetotactic Bacterium in the Microaerobic Zone of a Fresh Water Sediment, *Applied and Environmental Microbiology*, *59*(8), 2397–2403.

Staniland, S., et al. (2008), Controlled cobalt doping of magnetosomes in vivo, *Nature Nanotechnology*, *3*(3), 158–162.

Takai, K., and K. Horikoshi (1999), Genetic diversity of archaea in deep-sea hydrothermal vent environments, *Genetics*, *152*(4), 1285–1297.

Teske, A., et al. (2002), Microbial diversity of hydrothermal sediments in the Guaymas Basin: Evidence for anaerobic methanotrophic communities, *Applied and Environmental Microbiology*, *68*(4), 1994–2007.

Thomas-Keprta, K. L., et al. (2000), Elongated prismatic magnetite crystals in ALH84001 carbonate globules: Potential Martian magnetofossils, *Geochimica Et Cosmochimica Acta*, *64*(23), 4049–4081.

Ullrich, S., et al. (2005), A hypervariable 130 kilobase genomic region of Magnetospirillum gryphiswaldense comprises a magnetosome island which undergoes frequent rearrangements during stationary growth, *Journal of Bacteriology*, *187*(21), 7176–7184.

Vali, H., and J. L. Kirschvink (1991), Observations of Magnetosome Organization, Surface Structure, and Iron Biomineralization of Undescribed Magnetic Bacteria: Evolutionary Speculations, in *Iron Biominerals*, edited by R. Blakemore, Plenum Press, New York, pp. 97–116.

Wahyudi, A. T., et al. (2001), Isolation of *Magnetospirillum magneticum* AMB-1 Mutants Defective in Bacterial Magnetic Particle Synthesis by Transposon Mutagenesis, *Applied Biochemistry and Biotechnology*, *91–3*, 147–154.

Wolfe, R. S., et al. (1987), A Capillary Racetrack Method for Isolation of Magnetotactic Bacteria, *FEMS Microbiology Ecology*, *45*(1), 31–35.

Yamazaki, T., et al. (1995), Nitrite Reductase from the Magnetotactic Bacterium *Magnetospirillum magnetotacticum* — a Novel Cytochrome-cd1 with Fe(II)-Nitrite Oxidoreductase Activity, *European Journal of Biochemistry*, *233*(2), 665–671.

Yoshino, T., and T. Matsunaga (2005), Development of efficient expression system for protein display on bacterial magnetic particles, *Biochemical and Biophysical Research Communications*, *338*(4), 1678–1681.